this will cause a much lower $^{187}Re/^{188}Os$ ratio than that of seawater. The Os isotope system of these materials can be used as a paleo-marine environmental tracer since the $^{187}Os/^{188}Os$ ratio cannot grow significantly due to its extremely low $^{187}Re/^{188}Os$ ratio.

1. INTRODUCTION

Osmium (Os), a platinum group element (PGE), is one of the least abundant elements on the earth's surface. Over the past 20 years, it has attracted considerable attention from geochemists due to the variability of its isotopic system, as the decay of ^{187}Re to ^{187}Os (half-life = 41.6 Gy, Smoliar et al., 1996) gives rise to subsequent variations in the Os isotopic composition. As a result of large Re–Os fractionation during geological processes, the Os isotope ratio becomes highly variable as compared to that of other isotopic systems. Consequently, the $^{187}Os/^{188}Os$ ratio is often employed as a potentially powerful isotopic tracer on material cycling in the surface environment (Ravizza et al., 1996; Sharma et al., 1997; Levasseur et al., 2000; Dalai et al., 2005). In addition, the ^{187}Re–^{187}Os system can also be applied as a geochronometer to organic-rich sedimentary rocks such as black shales (Ravizza and Turekian, 1989; Cohen et al., 1999; Selby and Creaser, 2003), sulfide minerals rich in Re such as molybdenite (Suzuki et al., 1993), and iron meteorites (Smoliar et al., 1996).

Despite the frequent utilization of ^{187}Re–^{187}Os, the geochemical behavior of Os in the surface environment, especially in marine environments, is largely unknown. This is because the Os concentration in seawater is extremely low, and the chemical treatment of its natural samples for mass spectroscopic analysis is not very straightforward due to the varied oxidation states of Os (Sharma et al., 1997; Levasseur et al., 1998; Woodhouse et al., 1999). Furthermore, the dissolved species and residence times of Os in marine environments are subject to debates (Levasseur et al., 1998; Oxburgh, 1998; Woodhouse et al., 1999).

On the other hand, it is widely known that both Re and Os are enriched in reducing sediment and that their concentrations correlate well with total organic carbon contents (Ravizza et al., 1991). It is considered that significant removal of these elements from seawater to sediment occurs in reducing marine environments. However, the removal mechanisms of Re and Os from seawater are not yet fully understood, and differences in the removal mechanisms of these two elements should induce large variations in the Re/Os ratio in sediments. So far, the geochemical behaviors of Re and Os have not been studied simultaneously by systematic experiments focusing on each chemical process. This study is, to our knowledge, the first report focusing on the removal of Re and Os from seawater to sediment and their chemical species in sediments by using two methods, namely, the multitracer technique and X-ray absorption fine structure (XAFS).

In this study, the multitracer technique, a carrier-free multi-radiotracer technique (Ambe et al., 1995; Ambe, 1996), was applied in order to understand the behaviors of Re and Os in seawater–sediment systems. The main advantage of this technique is that it gives direct information on the partitioning of Re and Os at concentration levels similar to those found in the natural marine environment. The concentration of radioactive tracers, such as ^{183}Re and ^{185}Os, is about 10^{-13} M in each experimental system, while the concentration of Re or Os in natural seawater is about 4.4×10^{-11} M and 5.2×10^{-14} M, respectively (Peucker-Ehrenbrink and Ravizza, 2001). However, a significant limitation of this technique is that it provides no constraints on the speciation of Re and Os. Thus, the XAFS technique was applied to the current study so that it can provide direct information on the chemical states of Re and Os incorporated within the sediment prepared in laboratory experiments. Both XANES and EXAFS can provide direct constraints on the oxidation state and local coordination environment (such as the neighboring atom and interatomic distance), respectively. However, the relatively lower sensitivity of this method required working at concentration levels of about 6–7 orders of magnitude higher than that found in the natural marine environment. In this combined study, the reasonable coherence of the results from the two approaches indicates that the constraints on Re and/or Os speciation obtained at a higher concentration can be reasonably extended to the much lower levels found in nature.

Here, these two methods are applied to several chemical processes during the removal of Re and Os to sediments in laboratory experiments. A conceptual diagram showing the purposes of individual experiments and their mutual relationship is given in Fig. 1. The experimental process and the results of the two approaches will be dealt with by dividing these into two sections and combining the results of both types of experiments in Section 4.

2. XAFS STUDY

In this chapter, the chemical speciation of Re and Os in sediments, such as their oxidation states and coordinate environments, is discussed based on XAFS.

2.1. XAFS experiments

The Re reference materials for XAFS analysis, namely, ReO_4^- solution, ReO_2, ReS_2, and Re metal, were obtained commercially. The osmium tetraoxide solution (OsO_4), $(NH_4)_2OsCl_6$, $OsCl_3$, $OsO_2{\cdot}nH_2O$, OsS_2, and Os metal were used as Os reference materials. Perrhenate (ReO_4^-), OsO_4, and $(NH_4)_2OsCl_6$ were purchased from Kanto Chemical Co. Ltd. By adding OH^-, $OsO_2{\cdot}nH_2O$ was synthesized from $OsCl_6^{2-}$ (Cotton and Wilkinson, 1987). For Os sulfide reference material, erlichmanite (OsS_2) was synthesized by following a previously reported procedure (Hayashi et al., 2000). All of the other reference materials were purchased from Rare Metallic Co. Ltd.

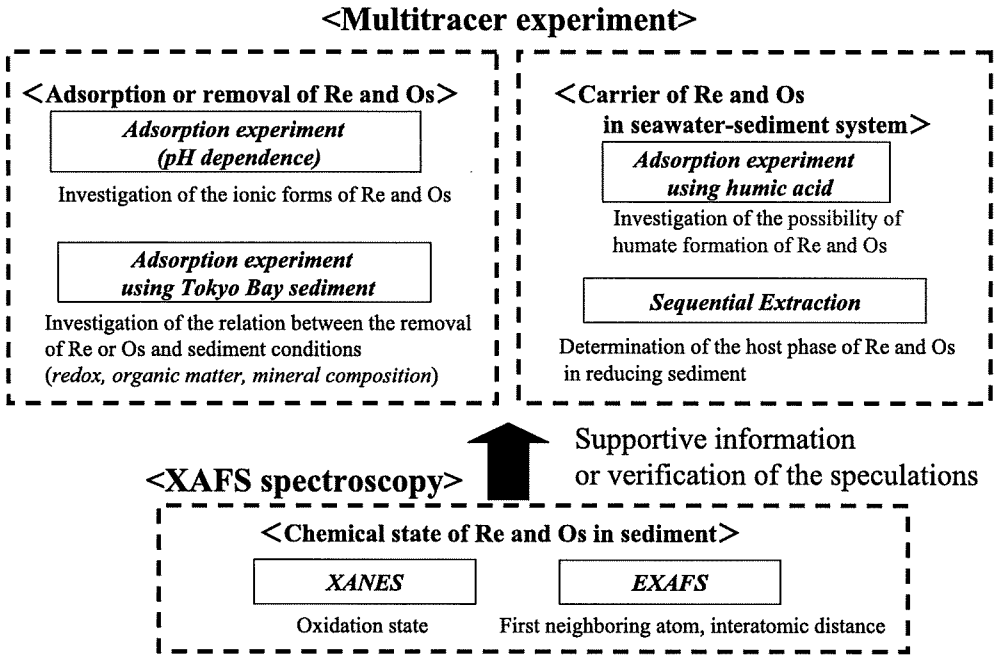

Fig. 1. Conceptual diagram for the purpose of individual experiments and the relation between each experiment.

The solid reference materials were diluted to 1 wt% by adding boron nitride or SiO_2 powder before pressing them into pellets. The sediment sample employed in this study was recovered from Tokyo Bay (N35°36.6′, E140°01.4′; 10 m depth). The sediment contained a high amount of organic C (2.07%) which was measured using a CHNS/O analyzer (Perkin Elmer 2400II). The other chemical composition of the sediment is shown in Appendix A. In order to investigate the effect of redox conditions on the oxidation states of Re and Os, untreated sediment (reducing) and air-dried sediment (oxic) were prepared (see Section 3.3.1). The weighed untreated or air-dried Tokyo Bay sediment (4.0 g) was flooded with 7.0 g of artificial seawater (see the Appendix A for the chemical composition) containing ReO_4^- (125 mg/dm^3) and either $OsCl_6^{2-}$ (62.5 mg/dm^3) or OsO_4 (250 mg/dm^3) in a polystyrene beaker with a cap. The beaker was then shaken for 2 weeks. In order to promote reduction, glucose (0.5 wt%) was added to the aqueous phase for some of the experimental systems (Rudolph et al., 1996). Here, $OsCl_6^{2-}$ and/or OsO_4 were used as the initial Os species in the artificial seawater, since they have been proposed to be the main Os species in seawater according to Koide et al. (1991), Brookins (1988). On the other hand, ReO_4^- was used as Re dissolved species in seawater (Brookins, 1988; Colodner et al., 1993, 1995). After incubation, the pH and Eh of the experimental system were measured using a glass electrode (Horiba, D-51) and a Pt electrode (Fujiwara, EHS-120). According to the partitioning coefficients of Re and Os obtained from the multitracer experiment, the concentrations of Re and Os in the sediments were estimated to be about 40 mg/kg and 100–400 mg/kg, respectively. The liquid phase was extracted as much as possible using a soil water sampler (Fujiwara, FV-448), and the sediment was packed in a polyethylene bag for XAFS measurements under an Ar atmosphere. After packing, the sediment samples were stored below −20 °C to prevent any chemical change during their storage until the XAFS measurement. The measurement and the analytical procedures of XAFS are shown in Appendix B.

2.2. Results of the XAFS study

The redox potentials of each experimental system for the XAFS experiment are summarized in Table 1. UTS (UnTreated Sediment) refers to untreated Tokyo Bay sediment incorporating Re and Os without the addition of glucose, while UTS-G (UnTreated Sediment with Glucose) indicates that with glucose. ADS (Air-Dried Sediment) indicates the air-dried Tokyo Bay sediment system without glucose. For Os in untreated sediment systems, three samples were prepared for each of UTS-G (OsO_4) and UTS-G ($OsCl_6^{2-}$), and the most and least reducing samples among the three was used for the XAFS measurement. The OsO_4 and $OsCl_6^{2-}$ in the parentheses show the initial Os species in the sorption study for XAFS measurement. Significant Eh decreases induced by microbial activity were observed for the untreated sediment systems. The pH decrease, with the progress of reducing conditions, was also observed for the experimental systems using untreated and dried sediments. Similar pH decreases were thermodynamically calculated for natural reducing environments, such as the Black Sea (Van Cappellen and Wang, 1996). Since the Eh value depends on pH, a simple comparison among the raw Eh values of each sediment cannot reveal the intrinsic difference among the redox conditions of each sediment. Following Bohn (1971), Megonigal et al. (1993), the Eh value was corrected to Eh*, the Eh value at pH 8 in each system (Eh*/mV = Eh/mV − (8-pH) × 59), in order to simplify the discussion. Table 1 includes the corrected Eh* and raw Eh–pH data. As shown in Table 1, Eh* in glucose-free or

Table 1
Eh–pH conditions of sediment samples (Tokyo Bay sediment) after 2 weeks of incubation for the XAFS measurement

Sample	Initial state	Sediment	Glucose (wt%)	pH	Eh (mV)	Eh* (mV)
Rhenium						
UTS-G (ReO_4-)	ReO_4^-	Untreated	0.5	5.2	−108	−273
UTS (ReO_4-)	ReO_4^-	Untreated	0.0	4.3	345	127
Osmium						
UTS-G1 ($OsCl_6^{2-}$)	$OsCl_6^{2-}$	Untreated	0.5	5.4	−35	−188
UTS-G2 ($OsCl_6^{2-}$)	$OsCl_6^{2-}$	Untreated	0.5	6.0	−127	−245
UTS-G1 (OsO_4)	OsO_4	Untreated	0.5	5.0	27	−150
UTS-G2 (OsO_4)	OsO_4	Untreated	0.5	4.9	−120	−303
ADS ($OsCl_6^{2-}$)	$OsCl_6^{2-}$	Air-dried	0.0	7.4	393	357
ADS (OsO_4)	OsO_4	Air-dried	0.0	7.2	422	374

Glucose was added to the aqueous phase of the seawater–sediment system to promote a reducing condition. The initial pH was adjusted to 8.0, which decreased with the progress of microbial-mediated reduction as described in Van Cappellen and Wang (1996).

air-dried sediment systems did not significantly decrease after incubation for 2 weeks.

The loading levels of Re and Os in artificial seawater were about 6–7 orders of magnitude higher than those in natural seawater. Therefore, there is the possibility that the speciation of Re and Os by XAFS does not reflect the natural speciation of both elements. However, as described in subsequent sections, the results of XAFS are likely to be reasonable because (i) the speciation by XAFS is consistent with the results of the distribution study using the multitracer technique, and (ii) the distribution ratios of Re and Os tracers are similar to those observed in nature.

2.2.1. XANES spectra for Re

Re L_{III}-edge XANES spectra of some reference materials and Re adsorbed on the sediment, along with the spectrum for Re in the artificial seawater recovered from the sediment, are shown in Fig. 2. As the oxidation state of Re becomes larger, the spectra of reference materials show that the absorption edge shifts to higher energy. This phenomenon (chemical shift) is commonly observed with many elements; it can be explained by the larger attraction forces between a nuclei and an inner electron for the ion at a higher oxidation state (Iida, 2000). Therefore, the oxidation state of Re adsorbed on sediments can be obtained from its peak energy by comparing it with that of the reference materials.

The XANES spectra of Re adsorbed on sediments and in the artificial seawater were quite similar to those of ReO_4^- in terms of the peak energy and spectral shape (Fig. 2). These results suggest that even under highly reducing conditions, not all Re was reduced as seen in the sample UTS-G (ReO_4^-). However, the peak energy of this sample shifted to a slightly lower energy than those of ReO_4^- and UTS (ReO_4^-). This result indicates that the redox condition of this sample ($Eh^* = -273$ mV, measured $Eh = -108$ mV at pH 5.2) reached the theoretical reducing potential of the ReO_4^-/ReO_2 couple ($Eh = -235$ mV at pH 8 and total $Re = 10^{-6}$ M: Brookins, 1988). The observation that the reduction of ReO_4^- to lower stable oxidation states, such as ReO_2 (or other tetravalent Re species), was not completed under highly reducing condition (our S K-edge XANES study shows that the main S species in UTS-G is sulfide) which indicates that the reduction process of ReO_4^- is relatively slow. At the least, the reduction of ReO_4^- cannot be attained within 2 weeks, even if the redox potential is sufficiently decreased compared to the reducing potential of ReO_4^-.

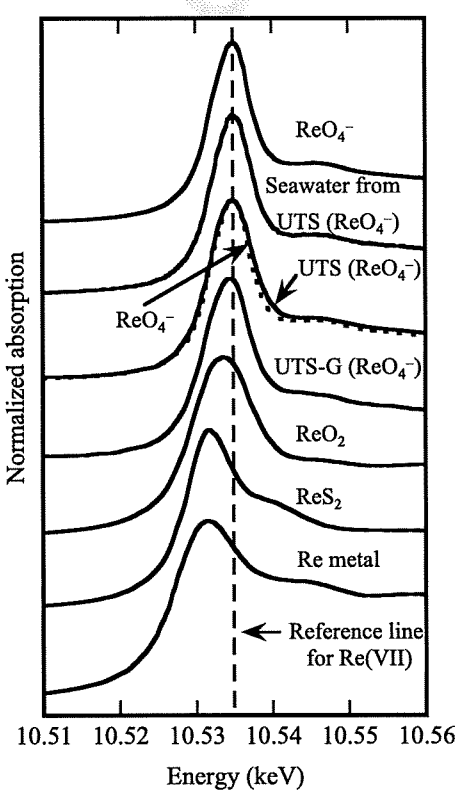

Fig. 2. Rhenium L_{III}-edge XANES spectra for reference materials (ReO_4^-, ReO_2, ReS_2, and Re metal), Re on sediment samples, and Re in artificial seawater recovered from the experimental system of the oxic sediment (UTS (ReO_4^-)). Following Bohn (1971) and Megonigal et al. (1993), the Eh values for each experiment were corrected to the values at pH 8 (Eh^*). The Eh^* and measured Eh–pH conditions for each sample are summarized in Table 1. The spectrum of ReO_4^- overlapped with that of UTS (ReO_4^-).

To investigate the contribution of Re(IV) in the sample UTS-G (ReO_4^-), the XANES spectrum for the sample was simulated by those of ReO_4^- and ReO_2 (Fig. 3). The

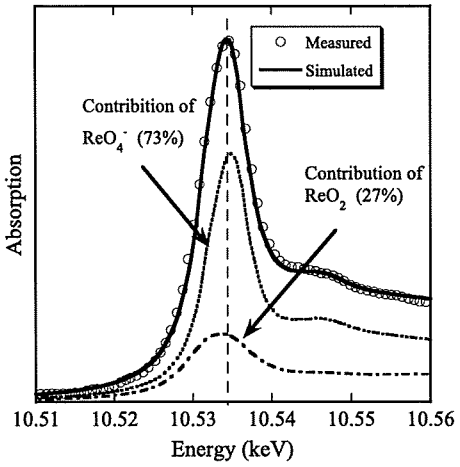

Fig. 3. Simulation of Re L_{III}-edge XANES by the spectra of ReO_2 and ReO_4^-. Open circle: sediment spectrum (UTS-G (ReO_4^-)); solid: fitted spectrum using the normalized spectra for ReO_4^- and ReO_2; dashed: the contributions of ReO_4^- and ReO_2.

simulation was able to explain the sample spectrum, and the contributions of ReO_4^- and ReO_2 were estimated to be 73% and 27%, respectively. This result suggests that the primary and secondary oxidation states of Re in the reducing sediments are Re(VII) and Re(IV), respectively.

2.2.2. XANES spectra for Os

Fig. 4 shows the Os L_{III}-edge XANES spectra of some reference materials and Os adsorbed on sediments. Two reducing sediment samples, a highly reducing one (UTS-G2) and a less reducing one (UTS-G1), were prepared.

As seen in Fig. 4, irrespective of the initial species (OsO_4 or $OsCl_6^{2-}$) introduced into the artificial seawater and the degree of the development of the reducing condition ($Eh^* < -100$ mV), the peak energies of the XANES spectra for Os adsorbed on all UTS-G series samples were similar to those of $OsCl_3$. This result indicates that Os adsorbed on the reducing sediment is mainly in a trivalent state. Since the initial oxidation state of Os was tetravalent or octavalent, it is confirmed that Os is incorporated into reducing sediments through reductive reactions.

On the other hand, the peak energy of Os adsorbed on air-dried sediment, ADS ($OsCl_6^{2-}$ or OsO_4), shifted to a higher energy and nearly coincided with that of $OsO_2{\cdot}nH_2O$. The Eh^* values of these sediments were about 350 mV, and, as with reducing sediment samples, significant differences between the energies of absorption peak related to the initial species ($OsCl_6^{2-}$ or OsO_4) were not observed in these samples. These results suggest that Os can be removed from seawater as Os(IV) at the first step. If the Os(VIII) oxyanion is assumed to be the dissolved species in seawater, chemical reduction is an important factor for the removal of Os. On the other hand, if Os(IV) is the dissolved species in seawater, chemical reduction is not important for the removal of Os under oxic conditions. Alternatively, ligand exchange from chlorine to oxygen can occur for Os(IV) without reduction. Following adsorption on sediment as Os(IV), Os(IV) can be reduced to Os(III) by diagenetic processes in the reducing sediment. This suggestion can be confirmed by the fact that the XANES spectra of the ADS series have a shoulder at the absorption peak of Os(III), showing that the ADS series contains Os(IV) and other species at lower oxidation states. The XANES spectra of the UTS-G series samples are dissimilar to those of $Os(II)S_2$ (Fig. 4), confirming that further reductive reactions from the Os(III) species to OsS_2 or Os metal could hardly proceed. The current S XANES study suggested that the main S species of the UTS series is sulfide (=98%, data not shown). Thus, Os sulfide species do not seem to be important (for any valence) in a reducing sediment system. Since the chemical shift was observed between the ADS series and UTS-G series samples, it is confirmed that the primary and secondary species of Os in marine sediments are Os(III) and Os(IV), respectively, and that the Os(III)/Os(IV) ratio may change as a function of the sediment redox condition.

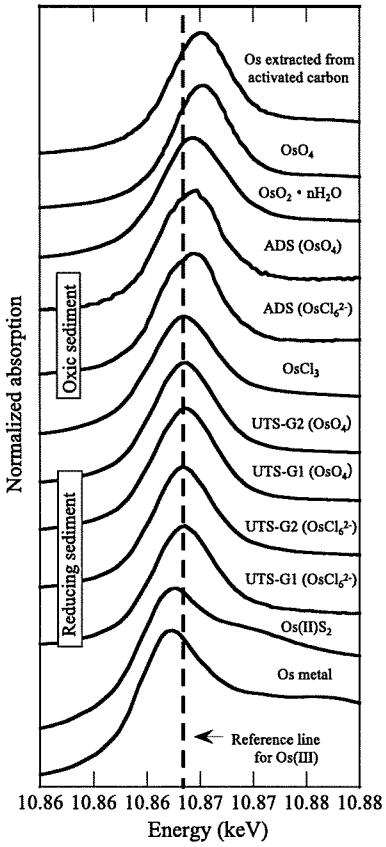

Fig. 4. Osmium L_{III}-edge XANES spectra for reference materials (OsO_4, $OsO_2{\cdot}nH_2O$, $OsCl_3$, OsS_2, and Os metal), Os extracted from activated carbon and Os on sediment samples. The Eh^* and measured Eh–pH conditions for each sample are summarized in Table 1.

2.2.3. EXAFS spectra of Os in sediments

Here, the EXAFS regions of Os in sediments are compared with those of some of the reference materials in order to obtain information on detailed species or specific structures of Os adsorbed on reducing sediments, UTS-G2 ($OsCl_6^{2-}$ or OsO_4). In addition, the EXAFS for reference

materials and UTS-G2 series samples were fitted using parameters generated by FEFF7.0.

Fig. 5 shows the k^3-weighted EXAFS function $\chi(k)$ of Os in the reducing sediments and some Os reference materials. The EXAFS functions of Os bound to Cl or S are similar to each other, but are clearly different from that of $OsO_2{\cdot}nH_2O$. The EXAFS function of $OsO_2{\cdot}nH_2O$ is characterized by its large amplitude observed in the lower k region ($k < 5$ Å^{-1}) as compared to that of $OsCl_6^{2-}$ or OsS_2. The structures in the EXAFS functions for both UTS-G2 samples are consistent with that of $OsO_2{\cdot}nH_2O$. As was seen in the XANES spectra, the EXAFS functions for Os in these two sediments are similar to each other in spite of their different initial chemical forms ($OsCl_6^{2-}$ or OsO_4).

Radial structural functions (RSF) of Os contained in the above sediments and Os reference materials are shown in Fig. 6. The $R+\Delta R$ (Å) of a first Fourier Transformation (FT) peak reflects the approximate interatomic distance (+ phase shift) between Os and the first neighboring scattering atom. The first FT peak of reference materials obviously follows the order of the ionic radii of coordinated

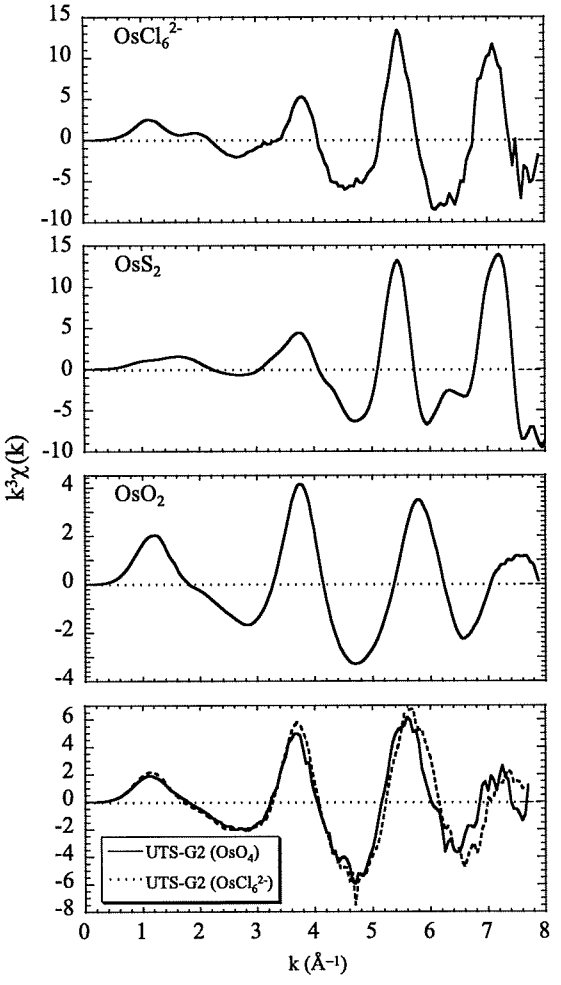

Fig. 5. The k^3-weighted Os L_{III}-edge EXAFS functions for reference materials ($OsCl_6^{2-}$, $OsO_2{\cdot}nH_2O$, and OsS_2) and sediment samples. The sediment samples are UTS-G2 (OsO_4) and UTS-G2 ($OsCl_6^{2-}$) in Fig. 3.

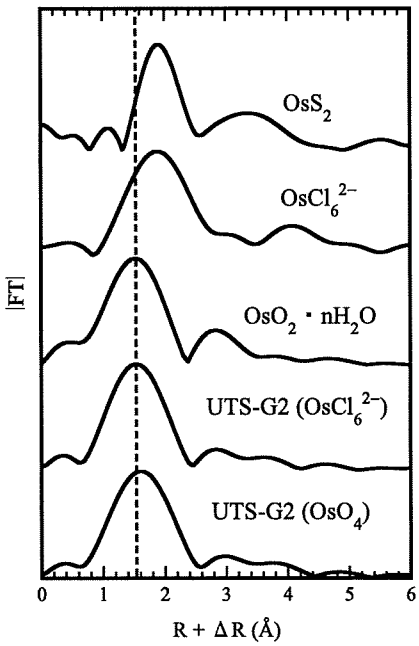

Fig. 6. Radial structure functions (RSF) for reference materials ($OsCl_6^{2-}$, $OsO_2{\cdot}nH_2O$, and OsS_2), UTS-G2 (OsO_4), and UTS-G2 ($OsCl_6^{2-}$). The phase shift was not corrected.

atoms ($O^{2-} < Cl^- < S^{2-}$; Shannon, 1976). These results suggest that the first neighboring atom of Os in the sediments can be distinguished by comparing the $R + \Delta R$ (Å) of the first peak with the reference materials. Since the $R + \Delta R$ (Å) of the first FT peak of Os in the sediment agrees with that of $OsO_2{\cdot}nH_2O$, the neighboring atom is likely to be oxygen.

The fitting parameters obtained here are shown in Table 2. To verify the quality of the simulation, reference materials were fitted in a way which is similar to Os in the sediments. The calculated interatomic distances for the Os–Cl ($OsCl_6^{2-}$), Os–O (OsO_2), and Os–S (OsS_2) bonds for the reference materials are 2.316, 1.963, and 2.350 Å, respectively ($N = 6$). These results are comparable with previous reports; the ideal interatomic distances for Os–Cl bond in $OsCl_6^{2-}$, Os–O bond in OsO_2, and Os–S bond in OsS_2 are 2.261, 1.961, and 2.351 Å, respectively (Boman, 1970; Cotton and Rice, 1977; Stingl et al., 1992). Therefore, the quality of the XAFS measurements and EXAFS analysis results using FEFF7.0 is acceptable. The fitting parameters for Os in the sediments, obtained by curve fitting, when the neighboring atom of Os was assumed to be Cl, O or S, are also shown in Table 2. When Cl or S was assumed to be the first neighboring atom of Os for the two sediment samples of UTS-G2 (OsO_4) and UTS-G2 ($OsCl_6^{2-}$), it becomes apparent that the calculated interatomic distances of Os–Cl (2.149–2.186 Å) and Os–S (2.168–2.217 Å) bonds were shorter than those expected from the analyses of reference materials. In contrast, when O was assumed to be the first neighboring atom of Os, the interatomic distances (1.984 or 2.017 Å) obtained for both sediments become comparable to that of the Os–O bond (1.961 Å) in a previous report (Boman, 1970).

Table 2
EXAFS fitting parameters using FEFF7.0 for $OsCl_6^{2-}$, $OsO_2{\cdot}nH_2O$, OsS_2, Os adsorbed on sediment from OsO_4 solution or $OsCl_6^{2-}$ solution

Sample	Shell	N	R(Å)	dE (eV)	DW	Residual (%)
$OsO_2 \cdot nH_2O$	Os–O	6	1.963 (0.004)	8.1 (0.4)	0.130 (0.006)	0.134
$OsCl_6^{2-}$	Os–Cl	6	2.316 (0.002)	8.1 (0.2)	0.061 (0.006)	0.208
OsS_2	Os–S	6	2.350 (0.003)	7.4 (0.4)	0.054 (0.004)	1.060
UTS-G2 (OsO_4)	Os–O	6	1.984 (0.002)	7.1 (0.2)	0.072 (0.005)	0.746
	Os–Cl	6	2.149 (0.003)	−4.7 (0.4)	0.117 (0.005)	0.329
	Os–S	6	2.168 (0.003)	−6.7 (0.3)	0.113 (0.005)	0.381
UTS-G2 ($OsCl_6^{2-}$)	Os–O	6	2.017 (0.004)	8.2 (0.4)	0.085 (0.008)	0.865
	Os–Cl	6	2.186 (0.003)	−2.7 (0.4)	0.125 (0.005)	0.699
	Os–S	6	2.217 (0.003)	−3.1 (0.4)	0.120 (0.005)	0.266

The first neighboring atom of Os in the sediments was assumed to be O, Cl, and S. N, coordination number fixed at 6 in this simulation; R (Å), interatomic distance; dE: threshold E_0 shift in eV; DW, Debye–Waller factor. The least squares precisions are given in parentheses. The accuracy of the fitted parameters was estimated to be generally ±0.02 for R (Å), and ±20% for DW (O'Day et al., 1994).

The EXAFS results reveal that the first neighboring atom of Os in the sediment is O and that the interatomic distance of the Os–O bond ranges from 1.984 to 2.017 Å. A slightly larger Os–O distance than OsO_2 (1.961 Å) suggests that Os(III)–O bonding is formed in the sediments because the ionic radius (r) generally becomes longer at a lower oxidation state ($r_{Os(IV)} < r_{Os(III)}$). This suggestion is partly supported by the XANES study, which indicates that Os(III) and Os(IV) coexist in these sediment systems, though a thorough confirmation of this result is not possible because Os_2O_3 is poorly characterized in the literature.

3. MULTITRACER STUDY

In this chapter, (i) the ionic forms of dissolved Re and Os in artificial seawater, (ii) Re and Os removal from artificial seawater to various sediments (untreated-, dried-, burnt-, and oxidized-sediments), (iii) the possibility of humate formation for Re and Os, and (iv) the host phase of Re and Os in artificial seawater–sediment system are discussed using the multitracer technique.

3.1. Preparation of the multitracer

Various radioisotopes, including ^{183}Re and ^{185}Os in the multitracer, were produced by the nuclear fragmentation reaction between Au target and heavy ions (^{12}C, ^{14}N, or ^{16}O) accelerated by RIKEN Ring Cyclotron in Wako, Japan (Ambe et al., 1995). The Au foil irradiated with the heavy ions was dissolved with aqua regia.

From the Au target, ^{185}Os and ^{183}Re were recovered. Since Os is easily oxidized with nitric acid to a highly volatile and strongly oxidizing octavalent state, dissolution of the Au foil containing ^{185}Os isotopes was performed in a closed system using a rotary evaporator. An activated carbon column was connected between the evaporator and an aspirator in order to recover the volatile Os, and the Os was extracted from the activated carbon by boiling it with 30 wt% H_2O_2 at 100 °C. From the residual solution containing Au and other radioisotopes, Au (matrix element) was removed by solvent extraction with ethyl acetate. Rhenium-183 was obtained from the water phase through the anion exchange method. The final working solutions were then prepared by adding a few microliter of the original multitracer solution to the working solution (artificial seawater, humic acid solution, and MQ water) followed by pH adjustment in every experiment. The speciation of various elements, except for Re and Os, in the original multitracer solution was documented by Takahashi et al. (1997, 1999). The speciation of Re and Os in the initial solution will be discussed later.

3.2. Adsorption onto various adsorbents

In this section, the ionic forms of the Re and Os ions in artificial seawater are investigated by adsorption experiments. Combining the results of XANES, the species of Re and Os in artificial seawater are estimated.

3.2.1. Experimental process

The adsorption of Re and Os on several adsorbents, such as hematite (Rare Metallic Co. Ltd.), ferromanganese oxide prepared as a powder of ferromanganese nodules (JMn-1: Geological Survey of Japan), silica gel (Fuji Division Chemicals Ltd.), and anion exchange resin (AG1-X8: Bio-Rad Laboratories), were examined under a wide range of pH conditions. Each adsorbent (0.5 g) was mixed with 7.0 g of artificial seawater containing multitracer in a polystyrene beaker with cap. After adjusting the pH of the solution with a small amount of NaOH or HCl solution, the suspension was shaken for 30 min. After centrifugation, the supernatant was recovered by filtration (0.45 μm). The γ-ray spectrum of radioisotopes in the filtrate was recorded using a pure Ge detector (GEM15P, Seiko EG&G) coupled with a multichannel analyzer. The γ-ray peaks were assigned to each radioisotope based on their half-lives and the energies of the photoelectric peaks. The peak area was computed using a routine program. The dissolved fraction of each element was calculated by comparison with a standard solution containing an identical amount of the multitracer, while the dissolved percentage of a radioisotope (R) was calculated by comparing the intensity of its peak for the sample (S_1) with that of the standard solution (S_0):

$$R(\%) = 100\, S_1/S_0 \quad (1)$$

The volumes of the sample and standard solution were kept constant at 3.0 ml to eliminate the effect of geometry on the Ge detector. Estimated from the radioactivity and the detection efficiency of the Ge detector, the concentrations of all of the radioisotopes in each experimental system were less than 10^{-13} M.

3.2.2. Adsorption onto various adsorbents

The adsorption of the multitracer on several adsorbents under various pH conditions is shown in Fig. 7. Without adsorbents, Re and Os were not removed, indicating that they are dissolved in the aqueous phase, and thus their removal by precipitation and adsorption on the walls of the polystyrene beaker can be ignored. After a contact time of 30 min, both Re and Os were significantly adsorbed on the anion exchange resin in the whole pH range, but their adsorption on silica, hematite, and ferromanganese oxide was minimal. On the other hand, Takahashi et al. (1999) reported that various cationic species were adsorbed on silica gel in a similar experimental system.

The surface charge of each adsorbent changes as a function of pH. Under acidic to neutral pH conditions, Mn and Fe oxides have positive charges, which turn into negative charges under neutral to basic pH conditions (Langmuir, 1997). On the other hand, the surface charges of silica and anion exchange resin are constantly negative and positive, respectively, under a wide pH region. The results of the adsorption experiment suggest that Re existed in an anionic form in artificial seawater. This result is consistent with previous studies that ReO_4^- is a stable species in the aqueous phase (Baes and Mesmer, 1986; Brookins, 1988). Furthermore, this suggestion is supported by XANES, the results of which reveal that Re was dissolved as ReO_4^- in artificial seawater (Fig. 2).

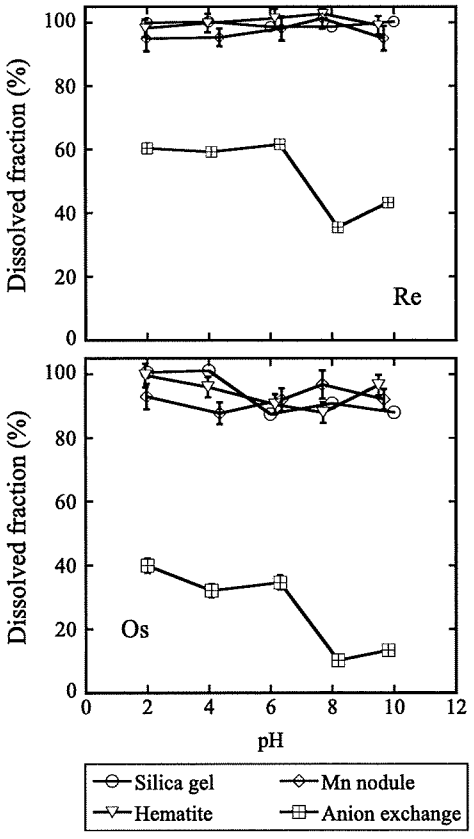

Fig. 7. Adsorption of Re and Os on various adsorbents (silica gel, ferromanganese oxide, hematite, and anion exchange resin). The pH_{ZPC} (point of zero charge) are 2.5, 2.5, and 6–8 for silica, ferromanganese oxide, and hematite, respectively (Langmuir, 1997).

The results of the adsorption experiment further suggest that Os is also dissolved in an anionic form in artificial seawater. Moreover, the XANES results show that Os extracted from activated carbon is octavalent (Fig. 4). Combining the results of XANES and the adsorption experiment using various adsorbents, the initial state of Os in artificial seawater used in the multitracer experiments was estimated to be the Os(VIII) anionic species, which are more specifically either $HOsO_5^-$ or $H_3OsO_6^-$.

3.3. Adsorption experiment onto Tokyo Bay sediments

In this section, the relationship between the removal behaviors of Re and/or Os on Tokyo Bay sediments and the condition of the sediments (such as redox potential, with or without organic matter, and mineral composition) using the multitracer technique is described.

3.3.1. Experimental process

The following sediment samples were prepared: (a) untreated sediment: containing a high proportion of organic carbon (2.07 wt%) which is un-oxygenated before the experiments, (b) air-dried sediment: containing a high proportion of organic carbon (2.07 wt%) which is well air-dried (well oxygenated at room temperature before the experiments), and (c-1) burnt sediment: burnt at 980 °C to decompose organic matter and sterilize microorganisms. "Oxidized sediment (c-2)" with 30 wt% H_2O_2 and 0.020 M HNO_3 for organic-free sediment was also prepared because the burning process decomposes the hydrous minerals, such as clay minerals, which are abundant in sediments and are important as sorption sites for metal ions. In experiments employing untreated sediment, the percentage of water content of the sediment was calculated in advance, and the weight ratio between the seawater and dry sediment was equalized among all four experimental systems. Weighed sediment (4.0 g) was flooded with artificial seawater (8.0 g) containing multitracer and adjusted to pH 8 in a polystyrene beaker with cap. In order to promote microbial activity (reducing condition), glucose (0.5 wt%) was added to the seawater of untreated- and dried-sediment systems following the method of Rudolph et al. (1996). The beaker was shaken constantly at 25 °C. At regular time intervals, the pH and Eh levels of the experimental system were measured, and 3.0 ml of seawater was recovered from the beaker to measure the γ-ray spectra after centrifugation. After the γ-ray measurements, each solution was returned to the original beaker.

3.3.2. Adsorption onto Tokyo Bay sediments

The results of the adsorption experiment using Tokyo Bay sediment are shown in Fig. 8, where the Eh* (and measured Eh–pH) change in each experimental system is also shown. In the untreated sediment system, Re was removed from artificial seawater to the sediment with an Eh decrease (Fig. 8a), but the dissolved fraction in the artificial seawater was still 81% at Eh* = −136 mV (measured Eh = −49 mV at pH 6.5). On the other hand, Re completely remained in the artificial seawater during the experimental period in the systems of dried-, burnt-, and oxidized- sediments (Figs. 8b, 8c-1, -2), where the Eh* value was larger than that in the untreated sediment (Eh* was 120, 470, and 348 mV for dried-, burnt-, and oxidized- sediments, respectively). That is, Re removal requires the development of reducing conditions in the presence of organic matter. However, a large amount of Re remained in the artificial seawater even in the untreated (reducing) sediment system. This is because the reducing potential of the ReO_4^-/ReO_2 couple is very low (e.g., reducing potential of Re(VII)/Re(IV) is about −274 mV at pH 8 and total Re = 10^{-8} M: Brookins, 1988), and the kinetics of ReO_4^- reduction may be slow, as indicated by the results of XAFS. Based on this adsorption experiment, it can be seen that the redox condition is an important factor in controlling the behavior of Re in a natural aquifer, and that Re is stable as a dissolved species (ReO_4^-) under reducing conditions, over a time scale of at least 2 weeks.

In contrast, a large amount of Os was removed from the artificial seawater to sediments in all systems (Fig. 8). For untreated-, dried-, and burnt-sediment systems, more than 80% of the total Os was incorporated in the sediments within 180 h (Fig. 8a–c1). The purpose of using untreated- and dried-sediment systems was to verify the removal behaviors of elements under highly reducing conditions with organic matter, and more oxic conditions with organic matter, respectively. In both experiments, Os was gradually removed from artificial seawater along with a microbially-mediated Eh* decrease. This result suggests that Os can be reduced to an insoluble form at a lower valence from the initial Os(VIII) dissolved species. This suggestion is somewhat reasonable because these sediments contain a

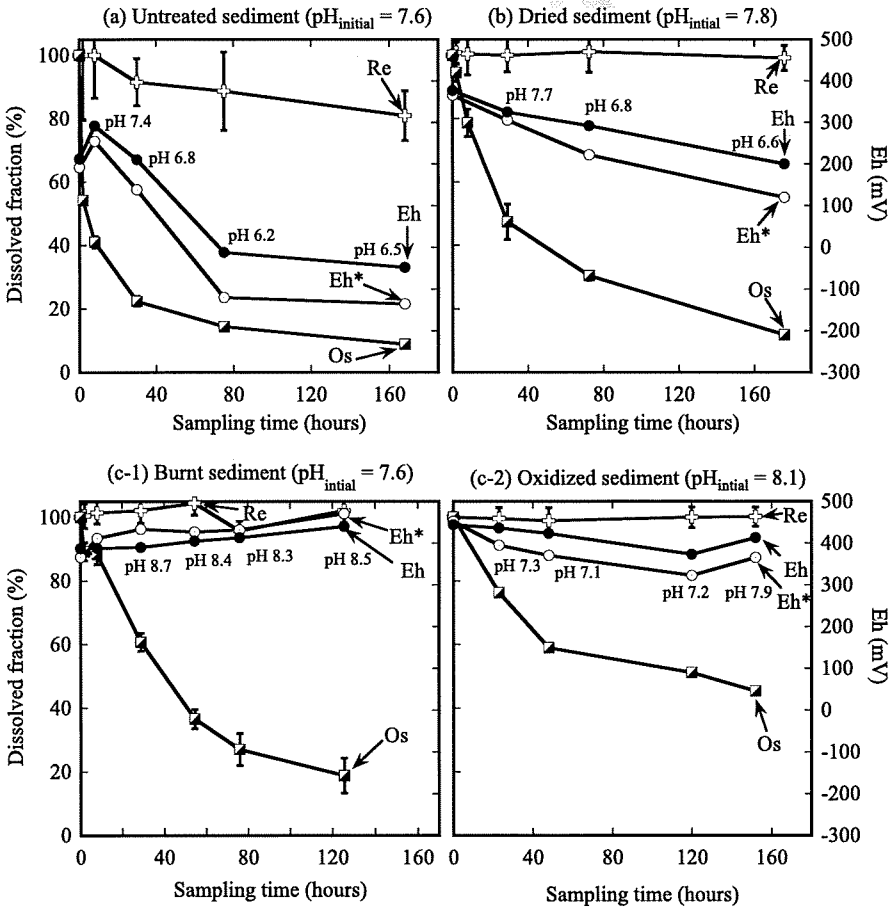

Fig. 8. Time-dependence of the removal of Re and Os from artificial seawater to sediment. The sediment samples are (a) untreated sediment, (b) dried sediment, (c-1) burnt sediment (980 °C), and (c-2) oxidized sediment (30% H_2O_2 and 0.02 M H_2NO_3). The removal patterns of Re and Os are shown as solid curves. The Eh* and measured Eh changes in each experimental system are also indicated by solid curves. The pH levels at the sampling times for each experimental system are shown in each figure. The average pH values for the systems were (a) 6.9, (b) 7.2, (c) 8.3, and (d) 7.4, respectively. For untreated sediment and dried sediment systems, the RSD (%) obtained from repeated experiments (n = 3) were less than 10%.

lot of reducing agents, such as organic matter. Moreover, the current XANES study also supports the results of these systems because it suggested that Os was reduced to Os(III) or Os(IV) and that it accumulated in the sediment (Fig. 4). In the presence of organic substances, the variation of redox conditions does not significantly affect the removal behavior of Os because organic matter itself acts as a reducing agent for Os.

In order to investigate the removal of Re and Os under oxic and organic-free conditions, burnt- and oxidized- sediment systems were prepared. In both systems of burnt- and oxidized-sediments (Fig. 8c-1, -2), a significant fraction of Os was also removed from artificial seawater to sediments. These accumulation processes may also be controlled by the reduction of initial Os(VIII). The fact that Os(VIII) species were not adsorbed onto hematite without reduction of Os (VIII) in the short time scale (Fig. 7) and that the reducing potential of Os(VIII)/Os(IV) was 374 mV (at pH 8 and total Os = 10^{-8} M: Brookins, 1988) indicate that initially added Os(VIII) species can be converted to more solid-reactive species in these experimental systems, probably as a result of the reduction of Os(VIII). In the current XANES study, it is confirmed that Os(VIII) was reduced to Os(IV), even in highly oxic air-dried sediments ($Eh^* = 374$ mV).

3.4. Rhenium and Os adsorption onto kaolinite: the effect of humic acid

From the results of the XAFS study and adsorption experiments using Tokyo Bay sediment, it was confirmed that reductive accumulation is relatively significant for both Re and Os in seawater–sediment systems. However, these results cannot provide detailed information on whether or not the reduced Re and Os are inorganically accumulated in marine sediments (adsorption onto minerals or incorporation into authigenic minerals) or are fixed on sediments by complexation with organic matter. In this section, the distribution behaviors of Re and Os between aqueous- and solid-phases were studied in the presence of humic acid (HA) to examine the possibility of their complexation with HA.

3.4.1. Experimental process

Rhenium and/or Os adsorption onto kaolinite in the absence and presence of HA was studied using the multitracer technique. Humic acid was extracted from paddy soil (Tochigi Prefecture, Japan) and was purified (Takahashi et al., 1995, 1998a). Kaolinite, purchased from Wako Chemicals Ltd., had a surface area of 7.5×10^2 m^2/g (Takahashi et al., 1998b). Weighed kaolinite (10 mg) was mixed with 5 ml of HA solution (30 mg/dm^3) or Milli-Q water in a polystyrene beaker. The ionic strength of the solution was adjusted to 0.020 M with NaCl, and its pH value was adjusted with a small amount of NaOH or HCl solution. In the metal–kaolinite–HA system, two types of experiments were conducted to check the effect of the order of injections of multitracer and HA: one type of experiment involves addition of the multitracer followed by HA after shaking for 5 days, while the other involves addition of HA followed by the multitracer. After shaking the solution for 10 days, the kaolinite was filtered out using a 0.45 μm membrane filter to recover the aqueous phase. The absorbance of the filtrate at 420 nm was compared with that of an initial HA solution (30 mg/dm^3) at a pH and ionic strength identical to each sample in order to determine the dissolved fraction of HA. One may think that seawater would make a better experimental aqueous phase for this study, since HA is pre-equilibrated with seawater in the natural marine environment. However, HA is readily coagulated in high ionic strength solutions, such as seawater (=0.7 M), and this situation is not good for observation of competition between adsorption onto kaolinite and humate formation in the aqueous phase; competition is needed in this experimental system to semi-quantitatively examine the effect of humate formation. Thus, a 0.020 M NaCl solution was applied in this experiment.

3.4.2. Adsorption in the absence and presence of humic acid

The pH dependence of adsorption of Re and Os on kaolinite in the absence and presence of HA accompanied by the pH dependence of HA distribution is shown in Fig. 9. Since HA is subjected to either precipitation or adsorption under acidic conditions, the dissolved fraction of HA was small, especially below pH 2. As the pH level increases,

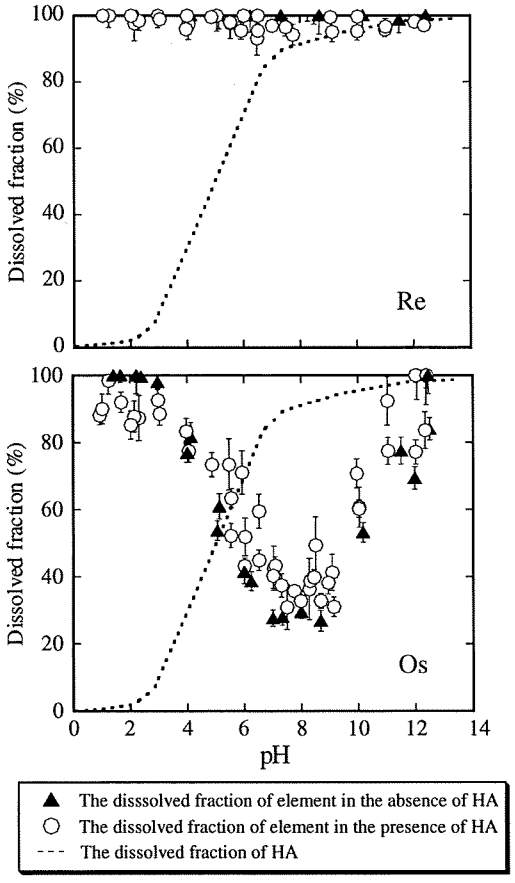

Fig. 9. The pH dependence of the dissolved fractions of Re and Os in contact with kaolinite in the absence and presence of HA. Kaolinite 10 mg; water 5.0 ml; initial concentration of HA: 30 mg/dm^3. The ionic strength was adjusted to 0.020 M with NaCl.

the HA molecule becomes negatively charged due to the deprotonation of the ligands, thereby promoting its dissolution. Under alkaline conditions, most of the HA was dissolved due to enhancement of the repulsion between dissociated HA and negatively charged kaolinite.

The adsorption of Re on kaolinite was not observed in the absence or presence of HA (Fig. 9). Irrespective of the order of injections of the multitracer and HA, the addition of HA did not influence the distribution of Re, suggesting that complexation with HA is not important for Re, at least not for ReO_4^-.

In both the binary (Os + kaolinite) and ternary (Os + kaolinite + HA) systems, the dissolved fraction of Os was minimal at neutral pH. These distribution patterns can be explained by the high reactivity of reduced Os, probably Os(III) and/or Os(IV) hydrolyzed species, with kaolinite surface around neutral pH (Fig. 9). Since the redox potential of the Os(VIII)/Os(IV) couple is high (e.g., 374 mV at pH 8 and $Os = 10^{-8}$ M: Brookins, 1988), Os(VIII) can be reduced to Os(IV) in water under ambient air condition. Under neutral to alkaline pH conditions ($5 < pH < 10$), the dissolved fraction of Os in the ternary system is slightly but systematically larger than that in the binary system. The binary and ternary system patterns intersect with each other at around pH 4. Under acidic conditions ($pH < 3$), although the dissolved fractions of both systems are close to 100%, the dissolved fraction of Os in the ternary system is slightly lower than that in the binary system. This result implies that a small amount of Os was fixed on kaolinite due to its complexation with HA adsorbed on the solid surface. Similarly, the dissolved fraction of HA binding to Os leads to an increase in the dissolved fraction of Os between pH 5 and 10 in the ternary system. If humate complex is dominant species both in the aqueous phase and on kaolinite, the distribution of the ion should be identical to that of HA (Takahashi et al., 1999). However, the dissolved fraction of Os was not identical to that of HA in this region, showing that there are other Os species adsorbed on the kaolnite and dissolved in the aqueous phase. It has been empirically confirmed that Os (and/or Re) is considerably enriched in organic-rich sediment, which is well correlated with total organic carbon (Ravizza et al., 1991). However, the result of this experiment is inconsistent with these observations, probably because Os enrichment requires the development of reducing conditions with the presence of organic matter.

3.5. Sequential extraction

The sediment that is rich in organic matter can be a sink of Re and Os under reducing marine environments (Ravizza et al., 1991). In addition, it was reported that a portion of Os dissolved by black shale weathering can be incorporated in ferromanganese oxides (Pierson-Wickmann et al., 2002). In order to identify the host phase of Re and Os in the sediment, sequential extraction experiments (Tessier et al., 1979; Koschinsky and Halbach, 1995) were performed for the reducing sediments (untreated Tokyo Bay sediment) containing multitracer in the adsorption experiments.

3.5.1. Experimental process

The leaching protocols followed those described in the studies of Tessier et al. (1979), Koschinsky and Halbach (1995) (see Appendix C for the details). The results show the six fractions of Re and Os including the aqueous phase in the system: (F1) seawater, (F2) exchangeable ion, (F3) carbonate, (F4) ferromanganese oxide, (F5) organic matter, and (F6) insoluble residue. In each extraction step, following the first separation of leaching solution (or artificial seawater), the residual sediment was washed with a few milliliter of leaching solution (or artificial seawater). The rinse solution was recovered by centrifugation and was mixed with the former. Gamma-ray analyses were performed on each fraction where the volume of each sample was constant at 25 ml, except for the insoluble residue (F6). The gamma-ray spectrum of the insoluble residue was then measured for the solid sample. The spectrum peak area for the residue was corrected by means of the correction factors obtained by comparing the detection efficiencies in the cases of solution (25 ml) and residual solid.

3.5.2. Results of sequential extraction

The sequential extraction results (Fig. 10) show the distribution of Re in the whole system in sorption experiments among the following phases: 70% in seawater (F1), 15% in exchangeable ion (F2), 2% in carbonate (F3), 5% in Fe–Mn oxide (F4), and 8% in organic matter (F5). The Re fractions belonging to F2- F5 may be in reduced forms, and based on thermodynamic calculations, it is thought that ReO_4^- reduction can occur under experimental conditions (pH 7.9, Eh = −191 mV). However, the results of sequential extraction also suggest that Re mainly exists as a dissolved species despite being partly incorporated in the reducing sediments.

Osmium was mainly found in the three fractions of organic matter (F5): ferromanganese oxides (F4), and seawater

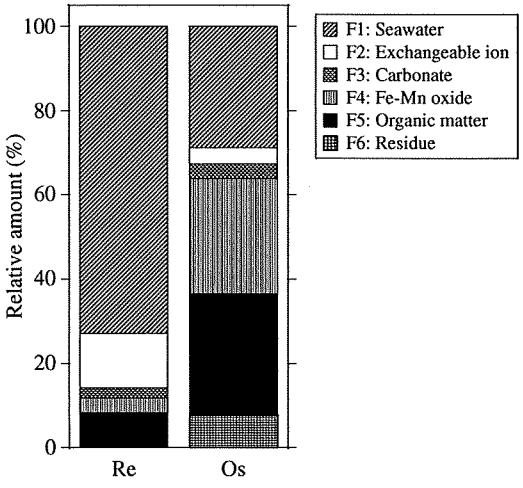

Fig. 10. Relative amount of Re and Os in six fractions (F1–F6) in the sequential extraction. The redox condition of the seawater–sediment system is pH 7.9 and Eh −191 mV. For the fractions recovered over 20%, RSD (%) calculated from repeated experiments ($n = 3$) was less than 20% of each value.

(F1). This result suggests that Os was incorporated in the reducing sediment as more than one chemical species. This suggestion is supported by the XANES study, which showed that the predominant Os species in marine sediments were Os(IV) and Os(III). Thirty percent and 10% of the total Os was found in ferromanganese oxides and the residual phase, respectively. Osmium incorporated in these phases may correspond to the hydrolyzed Os species at lower valences (III or IV), favoring sorption to mineral surfaces due to its large ionic potential. On the other hand, 30% of Os was incorporated in the organic matter fraction. This result implies the possibility that a fraction of Os can be complexed with organic matter. Although further study is needed to confirm the preference of Os as organic complexes, the distribution of Os in the organic matter fraction is supported by the adsorption study in the presence of HA (Section 3.4), where Os can form HA complexes to some degree.

It is possible that the re-oxidation of redox sensitive elements during each extraction step can occur in the sequential extraction experiments. Although the possibility of re-oxidation cannot be denied in the current experimental system, re-oxidation does not significantly affect the results, because (i) a large amount of Re is still retained as the Re(VII) species dissolved in artificial seawater in anoxic seawater–sediment systems (Figs. 3, 8-a, and 10), and (ii) if re-oxidation of Os occurred, the fractions of the exchangeable ion and carbonate should be larger. However, the fractions of ferromanganese oxides and organic matter still account for a large fraction of total Os (=collectively 60%). Hence, the results of the sequential extraction experiments in this study may be acceptable.

4. DISCUSSION

In this chapter, the geochemical behaviors of Re and Os in a marine environment are discussed by combining the results of the two types of experiments, which are then compared with the results of the behavior of Re and Os in a natural seawater–sediment system reported in previous studies. The understanding of Re/Os fractionation in various redox marine environments is also extended.

4.1. The geochemical behavior of Re in a seawater–sediment system

The conservative behavior of Re in a natural marine environment was reported by Anbar et al. (1992) and Colodner et al. (1993). They revealed that the Re concentration in seawater is constant throughout the water column, and that dissolved Re cannot be adsorbed onto suspended particles. On the other hand, many studies dealing with marine sediments have also pointed out that Re is highly enriched in organic-rich reducing sediments (Ravizza et al., 1991; Crusius et al., 1996; Cohen et al., 1999; Selby and Creaser, 2003). These reports are well consistent with the current laboratory results. In the current study's oxic experimental systems, Re showed conservative behavior: for instance, (i) the adsorption of ReO_4^- on various minerals was not observed, (ii) ReO_4^- did not interact with humic acid, and (iii) the ReO_4^- form was kept in the seawater–sediment system for 2 weeks. On the other hand, Re was enriched in organic-rich reducing sediment along with the development of a reducing condition in the adsorption study using untreated Tokyo Bay sediment and sequential extraction (Figs. 8a and 10). These results obviously suggest that Re removal can be controlled by chemical reduction. The XANES study robustly supports the reductive removal of Re as it suggests that Re incorporated in the reducing sediment within 2 weeks was partly reduced to lower oxidation states (Fig. 2). The Re XANES simulation with ReO_4^- and ReO_2 showed that the contributions to total Re in the reducing sediment from ReO_4^- and ReO_2 are 73% and 27%, respectively (Fig. 3). Although complete ReO_4^- reduction was not attained during the 2-week time frame [reducing potential of experimental system: $Eh^* = -273$ mV (or $Eh = -108$ mV at pH 5.2); reducing potential of ReO_4^-/ReO_2 couple: $Eh = -235$ mV at pH 8 and total $Re = 10^{-6}$ M: Brookins, 1988], this speciation is likely to be consistent with Re in the natural marine environment. Colodner et al. (1993) reported that dissolved Re can exist in the porewater of both oxic and reducing sediments. The fact that the distribution behavior and speciation of Re yielded by the multitracer and XANES studies are similar to those observed in nature indicates that ReO_4^- is a predominant Re species in reducing seawater–sediment system, even under sulfidic conditions. It can be thought that ReO_4^- reduction proceeds very slowly, even if the reducing potential of the experimental system reaches that of the ReO_4^-/ReO_2 couple. At the least, complete reduction was not attained within the given 2-week laboratory time scale. The slow reduction mechanism of Re was previously proposed by Crusius and Thomson (2000), Sundby et al. (2004). Based on the sediment-core study, they explained that the kinetics of Re accumulation can be controlled by a proposed multistep reduction mechanism in which, to a greater extent, longer times are required for the accumulation of Re in the sediment. The possible slow reduction mechanism in our experimental system can be confirmed by comparing the oxidation states of Re and S. Based on the reducing potentials of Re and S and the current S XANES study, (i) the reducing potential of the ReO_4^-/ReO_2 couple (-235 mV at pH 8 and total $Re = 10^{-6}$ M: Brookins, 1988) is higher than that of sulfate reduction (the reducing potential of SO_4^{2-}/HS^- is -305 mV at pH 8 and total dissolved S concentration is assumed to be 10^{-3} M: Brookins, 1988) and (ii) the current S XANES study suggests that the main S species in reducing sediments (UDS-G series) is sulfide (=98%). The fact that Re(IV) was not formed under the Eh condition where sulfide can be formed strongly suggests that the reduction of ReO_4^- to Re(IV) is slow.

Although the resistance of ReO_4^- to chemical reduction, the low reactivity of hydrated ReO_4^- ion with the oxide surface and the binding site of organic substances all cause the conservative behavior of Re in the seawater–sediment system, it was experimentally revealed in the current study that it is primarily chemical reduction that affects the accumulation of Re in the marine environment.

4.2. The geochemical behavior of Os in a seawater–sediment system

There are only a few previous studies which discussed the removal mechanism of Os in chemical terms (Koide et al., 1991; Woodhouse et al., 1999; Levasseur et al., 2000). All of these studies described the geochemical behavior of Os based on analyses of natural sediments or seawater with thermodynamic calculations. Here, the removal mechanism of Os is discussed by combining the current experimental results and the knowledge gained from previous reports.

Osmium is also known to be enriched with organic-rich reducing sediment (Ravizza et al., 1991; Cohen et al., 1999; Selby and Creaser, 2003). This empirical fact together with the thermodynamically expected Os dissolved species, Os(VIII) oxyanion, led Os geochemists to suggest that Os accumulates through reductive reaction (Woodhouse et al., 1999; Dalai et al., 2005). Based on seawater analyses, Levasseur et al. (1998) proposed that the geochemical behavior of Os can be controlled by inert organic matter, and that it can be conservative in marine environments. The current laboratory experiments are consistent with these previous suggestions. For instance, Os gradually and significantly accumulated into organic-rich sediments along with the development of a reducing condition (Figs. 8a, b and 10). This result indicates that Os can be incorporated in the sediments as a result of reduction from Os(VIII)-dissolved species. The reductive accumulation of Os is confirmed by the current XANES study (see Section 2.2.2 and Fig. 4). In addition, the distribution study using HA suggests that the aqueous behavior of Os was partly affected by HA. This distribution study also implies that there was another Os species in this experimental system, likely the Os hydrolysis species. In sequential extraction, it can also be seen that there are more than one Os species in seawater–sediment systems: one is in the organic-matter phase, and the other is in the Fe–Mn oxide or residual phase. The inference that there are more than one Os species in the seawater–sediment system is robustly confirmed by the Os XANES study. The results of XANES reveal that the Os incorporated in the reducing sediment was mainly in a trivalent state, and Os in the oxic (air-dried) sediment was mainly in a tetravalent state (Fig. 4). These results clearly suggest that the primary and secondary Os species in marine sediments are Os(III) and Os(IV), respectively, and that the Os(III)/Os(IV) ratio can change along with the variation of redox conditions.

If Os is dissolved in seawater as the Os(VIII) oxyanion, a reductive reaction is important for Os removal in seawater–sediment systems. In this case, the reducing agent may not be restricted to organic matter in seawater because Os(VIII) has a highly oxidizing property. For example, Mn(II) or Fe(II) may also play the role of a reducing agent for Os(VIII) in a natural oxic marine environment. In the current experimental systems, Os was readily removed from the artificial seawater to sediments even in the absence of organic matter (Fig. 8c-1, -2). The Os XANES result suggests that Os was reduced from the initial Os(VIII) to Os(IV) species even in oxic sediments (ADS series: $Eh^* = 357$ and 374 mV), and the results can be reasonably explained by previous thermodynamic estimations (Brookins, 1988). On the other hand, in the case where $OsCl_6^{2-}$ is assumed to be the Os dissolved species in seawater, initially coordinated Cl can be replaced by O through hydrolysis during the removal process, as confirmed by the EXAFS data (Figs. 5 and 6, and Table 2). Reduced Os from Os(VIII) to Os(IV) and/or initially dissolved $OsCl_6^{2-}$ is readily subjected to hydrolysis and adsorbed onto the mineral surfaces, or it may accumulate with the precipitation of authigenic minerals under relatively oxic conditions (e.g., Figs. 8c-1, -2, and 9). In nature, it has been reported that Os can be enriched in authigenic sediments (minerals), such as ferromanganese oxides, in oxic marine environments (Palmer et al., 1988; Koide et al., 1991; McDaniel et al., 2004). This accumulation process can be explained by the reactivity of the hydrolyzed metal (III or IV) ion with the surface of solids, as described in the results of the sequential extraction.

Following first burial as Os(IV), Os(IV) can be reduced further to Os(III) along with the development of reducing conditions. During this step, organic matter can act as a principal reducing agent and as a carrier for Os, probably by complexation. The possibility of the formation of Os–organic complex was partly supported by the results of the distribution study using HA and sequential extraction. The current Os EXAFS study also provides supportive information for the speciation of Os in the reducing sediments; the EXAFS results suggest that the O atom is the first neighboring atom of Os in the reducing sediment and that the Os–O bond length is approximately 2.00 Å. If Os is actually bound by organic ligands in the reducing sediment, the O atom at the deprotonated ligand of organic matter such as carboxylate can be a main binding site of Os. Moreover, a slightly and systematically longer Os–O bond length (about 2.00 Å) than that of the available Os(IV) oxide reference material (about 1.96 Å) seems to indicate the possibility of an Os(III)–organic complex (see Section 2.2.3).

Osmium can be in various oxidation states in natural marine environments because of its redox sensitivity. In more detail, it is confirmed that the main oxidation states of Os in the seawater–sediment system are tri- and tetra-valent. These Os ions can be readily subjected to hydrolysis and adsorbed onto solid surfaces, and partly interact with organic matter as well. The geochemical behavior of Os is controlled by many processes (described above), and it can be readily incorporated onto marine sediment under various redox environments.

4.3. Rhenium and Os fractionation

Many studies have reported that both Re and Os are enriched in reducing sediment that contains a high proportion of organic carbon (Ravizza et al., 1991; Cohen et al., 1999; Selby and Creaser, 2003; McDaniel et al., 2004). Based on the current experiments, it is clear that the geochemical behaviors of Re and Os in the seawater–sediment system are not similar, although both elements tend to be enriched in organic-rich reducing sediments. Large fractionation between Re and Os likely occurs during removal from seawater

to sediment. In this chapter, the $^{187}Re/^{188}Os$ ratio of the reducing sediment in the adsorption experiment (Fig. 8a) is calculated, and the fractionation between Re and Os during their removal is discussed by comparing the calculated $^{187}Re/^{188}Os$ ratio with those of the geological materials. As a first step, the distribution coefficients (K) of Re and Os are calculated using the data obtained from the adsorption experiment (Fig. 8a, at 168 h). The equation of K is described below:

$$K = \frac{(100 - R)/W_{\text{sediment}}}{R/W_{\text{artificial seawater}}} \quad (2)$$

where $R(\%)$ is the dissolved fraction of the element in artificial seawater at the end of the experiments, and W is the weight of artificial seawater or sediments. The model $^{187}Re/^{188}Os$ in the sediment, $(^{187}Re/^{188}Os)_{sed}$, is calculated below:

$$\left(\frac{^{187}Re}{^{188}Os}\right)_{sed} = \left\{\frac{(C_{Re} \times F_{^{187}Re}/N_{^{187}Re}) \times A}{(C_{Os} \times F_{^{188}Os}/N_{^{188}Os}) \times A}\right\}^{*} \times \frac{K_{Re}}{K_{Os}} \quad (3)$$

where C is the concentration of Re or Os in natural seawater, F is the isotopic abundance of ^{187}Re or ^{188}Os in natural seawater, N is the atomic mass of ^{187}Re or ^{188}Os, A is Avogadro's number, and K is the distribution coefficient of Re or Os. In this equation, the term in larger brackets (*) denotes the isotopic abundance ratio between ^{187}Re and ^{188}Os in natural seawater. In practice, a previously reported $^{187}Re/^{188}Os$ ratio for natural seawater (=4270, Peucker-Ehrenbrink and Ravizza, 2001) was applied in this calculation.

Only the $^{187}Re/^{188}Os$ ratio for untreated sediment can be calculated because Re was not removed to sediment except in the case of untreated sediment in the current adsorption experiment (Fig. 8). When the detrital fraction of Re or Os is not considered, the $^{187}Re/^{188}Os$ ratio for reducing sediment ($Eh^{*} = -136$ mV, measured $Eh = -48$ mV at pH 6.5) derived from Re and Os removal from artificial seawater was estimated to be approximately 120, as shown by ▲ in Fig. 11. It was reported that $^{187}Re/^{188}Os$ variations in sediment rich in organic matter ranged from one hundred to several thousands (Ravizza et al., 1991; Cohen et al., 1999; Selby and Creaser, 2003). The calculated $^{187}Re/^{188}Os$ for untreated sediment falls within the $^{187}Re/^{188}Os$ range reported in previous studies, and is higher than that of continental detritus such as loess (10–50: Hattori et al., 2003), but is lower, by about one order of magnitude, than that of average seawater (4270: Peucker-Ehrenbrink and Ravizza, 2001). This fact confirms that a large amount of Re and Os in sediments is derived from seawater in anoxic marine environments, as well as large fractionations between Re and Os occurring during their removal from seawater to sediments. It is known that natural Mn nodules (and other authigenic minerals) have an extremely low $^{187}Re/^{188}Os$ (~1: McDaniel et al., 2004) ratio under oxic marine environments, compared with seawater and/or continental detritus. Consequently, the $^{187}Os/^{188}Os$ ratio is roughly equal to that for average seawater. However, the model $^{187}Re/^{188}Os$ ratio for the oxic sediment ($Eh^{*} =$ 120–470 mV) cannot be calculated because no Re removal was observed in these experiments. The $^{187}Re/^{188}Os$ ratio observed in natural oxic sediments or authigenic minerals can be explained by the current experimental results. That is, Re cannot be incorporated into solid phases under oxic conditions (most of Re in these sediments would be derived from detritus). On the other hand, Os can be readily removed to solid phases even under oxic conditions. Accordingly, the $^{187}Re/^{188}Os$ ratio of oxic sediments (and authigenic minerals) can be lower as the contribution of authigenic phases becomes larger in the sediment.

The current study's results confirm that the $^{187}Re/^{188}Os$ variations of marine sediments and sedimentary rocks under various redox conditions are controlled by whether Re can be incorporated into the sediment. Under a reducing environment as described above, Re can be incorporated to larger degree, which induces a high $^{187}Re/^{188}Os$ ratio in the sediment (Fig. 11). The higher $^{187}Re/^{188}Os$ ratio causes larger growth of the $^{187}Os/^{188}Os$ ratio in natural rocks. Hence, organic-rich sedimentary rocks, such as black shales, can be targeted for Re–Os dating. In contrast, since only Os can be removed under an oxic environment, and given that Re in these sediments (and authigenic minerals) is only derived from detritus, the $^{187}Re/^{188}Os$ of authigenic materials such as ferromanganese oxide is lower than that of continental detritus (Fig. 11). The Os isotope system of authigenic materials that occurs in an oxic marine environment can be used as a paleo-marine environmental tracer because the growth of $^{187}Os/^{188}Os$ is not prominent due to the lower $^{187}Re/^{188}Os$ ratio. This interpretation of $^{187}Re/^{188}Os$ variation in various marine environments should be kept in mind during the discussion of Re–Os isotope systems in various sediments and sedimentary rocks.

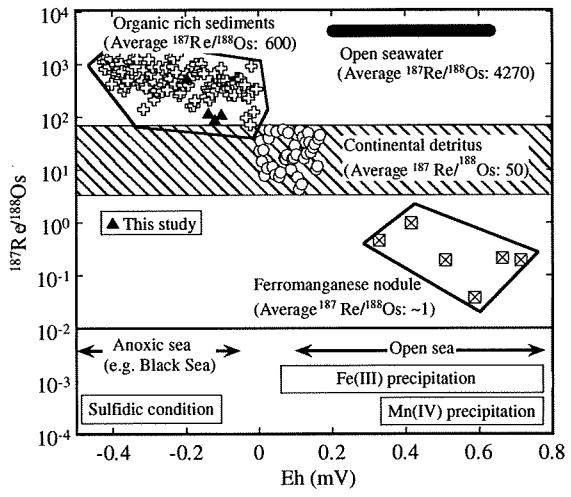

Fig. 11. Relationship between the redox condition in seawater and possible $^{187}Re/^{188}Os$ ratios in the sediments found in each environment. The estimated $^{187}Re/^{188}Os$ ratios based on our partitioning study were also plotted. The redox potential (or marine redox conditions) of each natural sample is assumed based on Brookins (1988), Langmuir (1997).

5. SUMMARY AND CONCLUSIONS

In this paper, the removal behaviors of Re and Os in a seawater–sediment system and Re/Os fractionation during

removal were studied by performing laboratory experiments using a multitracer technique and XAFS spectroscopy. A schematic diagram summarizing the accumulation processes and possible chemical species of Re and Os in the marine environment is shown in Fig. 12. The conclusions of this study are summarized as follows:

(a) The XAFS study revealed that Os incorporated in reducing sediments was mainly trivalent, and its first neighboring atom was O (the bond length is about 1.984–2.017 Å). Moreover, Os removed to dried sediments under oxic conditions was mainly in a tetravalent state. It is suggested that Os is first incorporated into the oxic sediments as Os(IV), mainly as the Os(IV) hydrolyzed species. Subsequently, Os(IV) can be reduced to Os(III) in organic-rich sediments with the development of a reducing environment. These results confirmed that Os(III) and Os(IV) coexist in seawater–sediment systems along with the variation of redox conditions.

(b) The ionic forms of Re and Os in artificial seawater were confirmed to be negatively charged. The current XANES study showed that Re in seawater can exist as ReO_4^- under various redox conditions, and that Os in water extracted from activated carbon is an octavalent species. If Os maintains its octavalent state in seawater during the contact time (30 min), its dissolved species may be anionic hydrolyzed species such as $HOsO_5^-$ or $H_3OsO_6^-$. This Os speciation seems to be correct in the highly oxic open ocean, but our study suggests that Os(IV) hydrolyzed species is more important in a seawater–sediment system.

(c) Rhenium and Os can be removed from artificial seawater to sediments with the development of reducing conditions, confirming that reductive removal is an important process for Re and Os. The removal of Os from the seawater to burnt sediment and organic-free sediment under oxic conditions was also observed, while Re was not removed from the seawater to the sediments under the same conditions. The removal process of Os seems to be controlled by several factors, such as reduction, hydrolysis, and organic complexation.

(d) The results of the adsorption experiment in the absence and presence of humic acid suggest that complexation with humic acid influences the distribution behavior of Os to some degree. Osmium also showed high affinity to an oxide surface, even in the presence of humic acid, suggesting the existence of hydrolyzed insoluble Os species.

(e) The sequential extraction showed that about 80% of Re remained in the seawater fraction after a 2-week incubation period despite a substantial Eh decrease. The XANES spectrum for Re in reducing sediment suggested that most Re existed as ReO_4^- in the reducing sediments. The XANES results also suggest that the reductive reaction of Re(VII) proceeds very slowly, probably due to its slow kinetics. Complete ReO_4^- reduction was not attained during the 2-week time scale in the laboratory experiments. Sequential

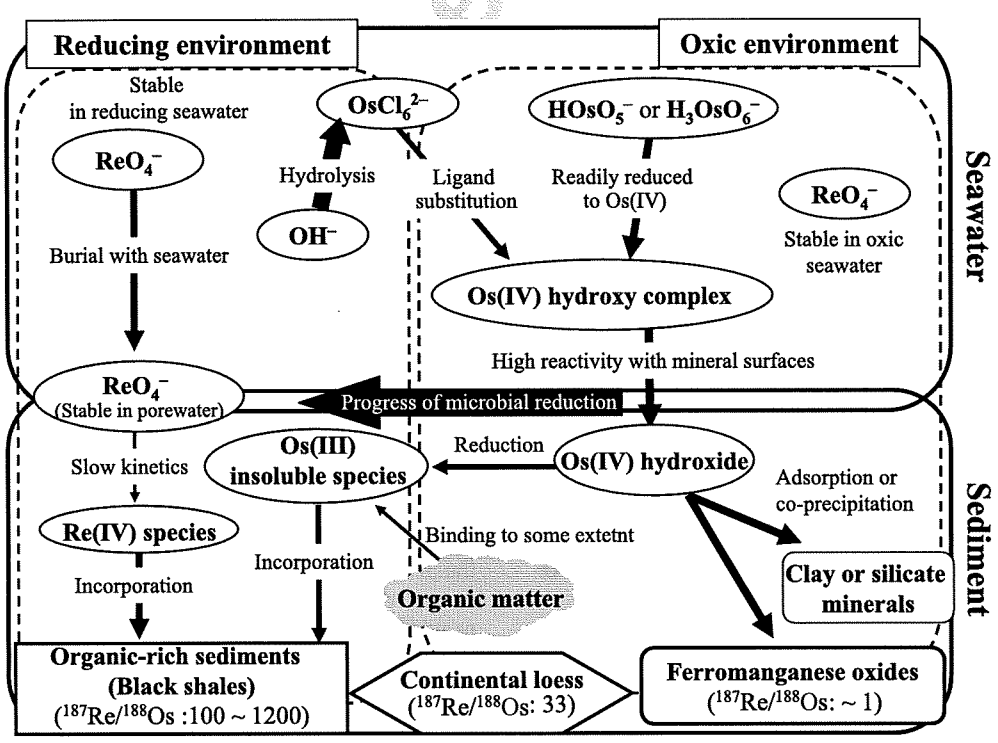

Fig. 12. Schematic diagram for the removal mechanism, possible chemical species of Re and Os, and variations of the $^{187}Re/^{188}Os$ ratio in geological samples in marine environments. The $^{187}Re/^{188}Os$ ratios of continental loess, ferromanganese oxides, and black shale followed the reports of Hattori et al. (2003), McDaniel et al. (2004), Selby and Creaser (2003), McDaniel et al. (2004), respectively.

extraction suggested that Os was distributed into three fractions, namely, seawater, Fe–Mn oxides, and organic matter. These results further suggest that Os assumes more than one species in a seawater–sediment system, which was also supported by the XAFS study. Osmium in the ferromanganese oxide and residual phases may be a hydrolyzed Os(III or IV) species favoring mineral surfaces due to its high ionic potential, while Os in the organic-phase may be Os(III) complexed with organic matter.

(f) Although Re is removed to sediments only under highly reducing condition in our experiments, the slow kinetics of Re reduction can inhibit the observation of Re removal under less reducing condition within the timescales of the experiments. Actually, Re can be removed under mildly reducing condition in natural marine environments (Crusius et al., 1996; Morford et al., 2007). Hence, we here conclude that reducing condition is needed for the removal of Re to sediments, while Os can be removed even under oxic condition as shown in our experiments. Thus, a high $^{187}Re/^{188}Os$ ratio can occur in reducing sediments, such as black shales. The high $^{187}Re/^{188}Os$ ratio makes black shales suitable for Re–Os dating due to the larger growth of $^{187}Re/^{188}Os$. In contrast, authigenic sediments (and minerals) under oxic environments can only enrich Os, which causes a much lower $^{187}Re/^{188}Os$ ratio than that of seawater. The osmium isotope system of these materials can be used as a paleo-marine environmental tracer because the $^{187}Os/^{188}Os$ ratio cannot grow significantly due to its extremely low $^{187}Re/^{188}Os$ ratio.

ACKNOWLEDGMENTS

The researchers would like to thank Mr. M. Ito and Ms. H. Mouri for their contributions to the experiment. They are likewise grateful to the Hiroshima University Radioisotope Center for their support of the study, and to Prof. K. Hayashi (Okayama University of Science) for synthesizing the OsS_2 sample. Three anonymous reviewers are also acknowledged for their thorough review and helpful comments. Finally, the researchers are very grateful to Dr. J. Crusius (AE of this paper) for his thoughtful and constructive comments. This study was supported by a Grant-in-Aid for Scientific Research from the Japan Society for the Promotion of Science and a fund from the Shimadzu Science Foundation. This study was performed with the approval of KEK (2002G243 and 2004G119) and SPring-8 (2001B0393-NX-np, 2004A0617-NXa-np, and 2005A0628-NXa-np).

APPENDIX A. ARTIFICIAL SEAWATER AND TOKYO BAY SEDIMENT

The chemical composition of artificial seawater followed that in the study of Tsunogai and Noriki (1983); Milli-Q water: 1000 g, NaCl: 23.5 g, $MgCl_2 \cdot 6H_2O$: 10.6 g, Na_2SO_4: 3.98 g, $CaCl_2 \cdot 2H_2O$: 1.48 g, $NaHCO_3$: 0.19 g.

The chemical composition determined by XRF for the Tokyo Bay sediment is as follows: SiO_2: 50.4 wt%; TiO_2: 0.6 wt%; Al_2O_3: 14.3 wt%; Fe_2O_3: 5.7 wt%; MnO: 0.09 wt/%; MgO: 2.6 wt%; CaO: 2.9 wt%; Na_2O: 3.99 wt%; K_2O: 1.6 wt%; P_2O_5: 0.12 wt%.

APPENDIX B. XAFS MEASUREMENT AND ANALYSIS

Rhenium L_{III}-edge XAFS spectra were measured at the beamline 12C in KEK-PF (Tsukuba, Japan) where a Si (111) double-crystal monochromater and a bent cylindrical mirror were employed to obtain monochromatic X-ray. Osmium L_{III}-edge XAFS spectra were obtained at the beamline BL01B1 in SPring-8 (Hyogo, Japan) equipped with a Si (111) double-crystal monochromater using two mirrors. The measurements were carried out at room temperature. The energy calibration was conducted for Re and Os L_{III}-edges with ReO_2 and $OsCl_3$, respectively. In order to obtain fluorescent XAFS spectra for the sediment samples, a 19-element Ge solid state detector (SSD) was employed and Al foil was placed between the sample and the detector to reduce the entry of X-ray fluorescence in SSD from major elements such as Fe and Mn in sediments. By taking repeated scans for most of the samples, a possible change of XAFS spectra due to the alteration of Os and Re species during XAFS measurements was checked. As a result, it was found that no appreciable change in the XAFS spectra was observed, and the repeated scans were averaged to obtain each XAFS spectrum.

In the case of fluorescence XAFS measurements by SSD, dead time corrections were made for the SSD counting. XANES and EXAFS analyses were performed using REX2000 Ver. 2.3 (Rigaku Co.). For the XANES data measured in fluorescence mode, the background absorption was subtracted using a linear function estimated from pre-edge region. On the other hand, the Victoreen equation was applied for the calculation of background absorption of the spectra obtained by the transmission mode. Following the subtraction of background, the spectra were normalized to absorption at the post-edge region. For the EXAFS region, after background correction and normalization, the smooth L_{III}-edge absorption of the free Os atom (μ_0) was removed using a spline curve. EXAFS function $\chi(k)$ was extracted from the XAFS spectrum by transforming incoming X-ray energy units (keV) to photo-electron wave number ($Å^{-1}$). Fourier transformation of k^3-weighted $\chi(k)$ function from k-space ($Å^{-1}$) to R-space (Å) was performed to obtain a radial structural function (RSF) in the k ($Å^{-1}$) range $3.25 < k < 7.05$ for all the Os samples. The k range used for the fourier transformation was determined based on the available k range for sediment samples. A Fourier inverse transformation was performed on the first shell of the RSF. The theoretical EXAFS function was fitted to an inversed k^3-weighted $\chi(k)$ function using parameters provided by FEFF7.0 (Zavinsky et al., 1995; Ankudinov and Rher, 1997). The EXAFS analysis provides the coordination number (N), the interatomic distance (R), the energy offset (dE), and the Debye–Waller factor (DW) for the first shell in this study. Following Stern (1993), the maximum number of parameters for curve fittings (N_{free}) were calculated ($N_{free} = 4$). Considering the coordination number of

Os standard materials ($OsCl_6^{2-}$ $OsO_2 \cdot nH_2O$, and OsS_2), the coordination number of Os in sediment was fixed at 6. Assessing the quality of each fitting, the *R*-factor, showing the difference between experimental and theoretical $\chi(k)$ functions, was utilized (Sakakibara et al., 2005).

APPENDIX C. PROTOCOLS OF SEQUENTIAL EXTRACTION

The protocols of sequential extraction basically followed those described in the studies of Tessier et al. (1979) and Koschinsky and Halbach (1995).

(1) Upon adsorption of the multitracer, the polystyrene beaker was centrifuged, and the seawater (F1) was recovered as much as possible. The residual sediment was air-dried and disaggregated in the beaker.
(2) An aliquot of sediment (0.8 g) was treated with 8 ml of 1.0 M sodium acetate at pH 8.0. The sample was shaken for 1 h at room temperature. The aqueous phase was separated by centrifugation. This step extracts easily exchangeable ions (F2).
(3) The residue from (2) was mixed with 8 ml of 1.0 M sodium acetate at pH 5.0 and was shaken for 10 h at room temperature. This step leaches the elements bound to the carbonate (F3).
(4) The residue from (3) was treated with 20 ml of 0.20 M ammonium oxalate (pH 3.5) and was shaken for 24 h at room temperature. This step extracts elements bound to the ferromanganese oxides (F4).
(5) The residue from (4) was mixed with 3 ml of 0.020 M HNO_3 and 5 ml of 30 wt% H_2O_2 (pH 2.0, adjusted with HNO_3), and was shaken at 60 °C until the vigorous reaction was terminated. Thirty wt% H_2O_2 (5 ml) was reloaded and shaken in the same way. The aqueous phase was recovered by centrifugation. After that, 5 ml of 3.2 M ammonium acetate (pH 2.0) was introduced into the residue and it was shaken for 1 h at room temperature. The liquid phase was separated by centrifugation and was mixed with the former. This step extracts elements bound to the organic matter (F5).
(6) The residue (F6) from (5) was air-dried.

REFERENCES

Ambe S., Chen S. Y., Ohkubo Y., Kobayashi Y., Maeda H., Iwamoto M., Yanokura M., Takematsu N., and Ambe F. (1995) "Multitracer" a new tracer technique—its principle, features, and application. *J. Radioanal. Nucl. Chem.* **195**, 297–303.

Ambe F. (1996) *The Multitracer, Its Application to Chemistry, Biochemistry, and Biology, RIKEN review*, vol. 13.

Anbar A. D., Creaser R. A., Papanastassiou D. A., and Wasserburg G. J. (1992) Rhenium in seawater: confirmation of generally conservative behavior. *Geochim. Cosmochim. Acta* **56**, 4099–4103.

Ankudinov A. L., and Rher J. J. (1997) Relativistic calculations of spin-dependent X-ray absorption spectra. *Phys. Rev. B* **56**, 1712–1716.

Baes C. F., Jr., and Mesmer R. E. (1986) *The Hydrolysis of Cations*. Krieger Rub. Com., Florida.

Bohn H. L. (1971) Redox potentials. *Soil Sci.* **112**, 39–45.

Boman C. E. (1970) Precision determination of the crystal structure of osmium dioxide. *Acta Chem. Scand.* **24**, 123–128.

Brookins D. G. (1988) *Eh–pH Diagrams for Geochemistry*. Springer, Berlin.

Cohen A. S., Coe A. L., Bartlett J. M., and Hawkesworth C. J. (1999) Precise Re–Os ages of organic-rich mudrocks and Os isotope composition of Jurassic seawater. *Earth Planet. Sci. Lett.* **167**, 159–173.

Cotton F. A., and Rice C. E. (1977) Structure of the high-temperature form of osmium(IV) chloride. *Inorg. Chem.* **16**, 1865–1867.

Cotton F. A., and Wilkinson G. (1987) *Advanced Inorganic Chemistry*, fourth ed. Wiley, New York.

Colodner D., Sachs J., Ravizza G., Turekian K. K., Edmond J., and Boyle E. (1993) The geochemical cycle of rhenium: a reconnaissance. *Earth Planet. Sci. Lett.* **117**, 205–221.

Colodner D., Edmond J., and Boyle E. (1995) Rhenium in Black Sea: comparison with molybdenum and uranium. *Earth Planet. Sci. Lett.* **131**, 1–15.

Crusius J., Calvert S. E., Pederson T. F., and Sage D. (1996) Rhenium and molybdenum enrichments in sediments as a indicators of oxic, suboxic and anoxic conditions of deposition. *Earth Planet. Sci. Lett.* **145**, 65–79.

Crusius J., and Thomson J. (2000) Comparative behavior of authigenic Re, U, and Mo during reoxidation and subsequent long-term burial in marine sediments. *Geochim. Cosmochim. Acta* **64**, 2233–2242.

Dalai T. K., Suzuki K., Minagawa M., and Nozaki Y. (2005) Variations in seawater osmium isotope composition since the last glacial maximum: A case study from Japan Sea. *Chem. Geol.* **220**, 303–314.

Hattori Y., Suzuki K., Honda M., and Shimizu H. (2003) Re–Os isotope systematics of the Taklimakan Desert sands, moraines and river sediments around the Taklimakan Desert, and of Tibetan soils. *Geochim. Cosmochim. Acta* **67**, 1195–1205.

Hayashi K., Serikawa D., Maeda N., Okamoto A., and Ikeuchi T. (2000) Microwave absorption materials - IV Preparation of the mixed layer structure phases, $Re_\chi Ta_{1-\chi} S_2$ and $Os_\chi Ta_{1-\chi} S_2$, and some electrical and magnetic properties. *J. Eur. Ceram. Soc.* **20**, 2735–2742.

Iida A. (2000) Instrumentation for μ-XRF at synchrotron sources. In *Microscopic X-ray Fluorescence Analysis*, (eds. K.H.A. Janssens, F.C.V. Adams and A. Rindby), p. 142. Wiley, Chichester.

Koide M., Goldberg E. D., Niemeyer S., Gerlach D., Hodge V., Bertine K. K., and Padova A. (1991) Osmium in marine sediments. *Geochim. Cosmochim. Acta* **55**, 1641–1648.

Koschinsky A., and Halbach P. (1995) Sequential leaching of marine ferromanganese precipitates: genetic implications. *Geochim. Cosmochim. Acta* **59**, 5113–5132.

Langmuir D. (1997) *Aqueous Environmental Geochemistry*. Prentice-Hall, New Jersey.

Levasseur S., Brick J.-L., and Allegre C. J. (1998) Direct measurement of femtomoles of osmium and the $^{187}Os/^{188}Os$ ratio in seawater. *Science* **282**, 272–274.

Levasseur S., Rachold V., Brick J.-L., and Allegre C. J. (2000) Osmium behaviour in estuaries: the Lena River example. *Earth Planet. Sci. Lett.* **177**, 227–235.

McDaniel D. K., Walker R. J., Hemming S. R., Horan M. F., Becker H., and Grauch R. I. (2004) Sources of osmium to modern oceans: New evidence from the ^{190}Pt-^{186}Os system. *Geochim. Cosmochim. Acta* **68**, 1243–1252.

Megonigal J. P., Patrick, Jr., W. H., and Faulkner S. P. (1993) Wetland identification in seasonally flooded forest soils: Soil morphology and redox dynamics. *Soil Sci. Soc. Am. J.* **57**, 140–149.

Morford J. L., Martin W. R., Kalnejais L. H., Francois R., Bothne M., and Karle I. M. (2007) Insights on geochemical cycling of U, Re and Mo from seasonal sampling in Boston Harbor, Massachusetts, USA. *Geochim. Cosmochim. Acta* **71**, 895–917.

O'Day P. A., Rehr J. J., Zabinsky S. J., and Brown G. E. (1994) Extended X-ray absorption fine structure (EXAFS) analysis of disorder and multiple scattering in complex crystalline solids. *J. Am. Chem. Soc.* **116**, 2938–2949.

Oxburgh R. (1998) Variations in the osmium isotope composition of sea water over the past 200,000 years. *Earth Planet. Sci. Lett.* **159**, 183–191.

Palmer M. R., Falkner K. K., Turekian K. K., and Calvert S. E. (1988) Sources of osmium isotopes in manganese nodules. *Geochim. Cosmochim. Acta* **52**, 1197–1202.

Peucker-Ehrenbrink B., and Ravizza G. (2001) The marine osmium isotope record. *Terra Nova* **12**, 205–219.

Pierson-Wickmann A.-C., Reisberg L., and France-Lanord C. (2002) Behavior of Re and Os during low-temperature alteration: Results from Himalayan soils and altered black shales. *Geochim. Cosmochim. Acta* **66**, 1539–1548.

Ravizza G., and Turekian K. K. (1989) Application of the $^{187}Re/^{188}Os$ system to black shale geochronometry. *Geochim. Cosmochim. Acta* **53**, 3257–3262.

Ravizza G., Turekian K. K., and Hay B. J. (1991) The geochemistry of rhenium and osmium in recent sediments from Black Sea. *Geochim. Cosmochim. Acta* **55**, 3741–3752.

Ravizza G., Martin C. E., German C. R., and Thompson G. (1996) Os isotopes as tracers in seafloor hydrothermal systems; metalliferous deposits from the TAG hydrothermal area, 26 degrees N Mid-Atlantic Ridge. *Earth Planet. Sci. Lett.* **138**, 105–119.

Rudolph J., Koschprreck M., and Conrad R. (1996) Oxidative and reductive microbial consumption of nitric oxide in a heathland soil. *Soil Biol. Biochem.* **28**, 1389–1396.

Sakakibara N., Takahashi Y., Okumura K., Hattori K. H., Yaita T., Suzuki K., and Shimizu H. (2005) Speciation of osmium in an iron meteorite and a platinum ore specimen based on X-ray absorption fine-structure spectroscopy. *Geochem. J.* **39**, 383–389.

Selby D., and Creaser R. A. (2003) Re–Os geochronology of organic-rich sediments: an evaluation of organic matter analysis. *Chem. Geol.* **200**, 225–240.

Shannon R. D. (1976) Revised effective ionic radii and systematic studies of interatomic distances in halides and chalcogenides. *Acta Cryst.* **A32**, 751–767.

Sharma M., Papanastassiou D. A., and Wasserburg G. J. (1997) The concentration and isotopic composition of osmium in the oceans. *Geochim. Cosmochim. Acta* **61**, 3287–3299.

Smoliar M. I., Walker R. J., and Morgan J. W. (1996) Re–Os ages of group IIA, IIIA IVA, and IVB iron meteorites. *Science* **271**, 1099–1102.

Stern E. A. (1993) Number of relevant independent points in X-ray absorption fine-structure spectra. *Phys. Rev. B* **48**, 9825–9827.

Stingl T., Mueller B., and Lutz H. D. (1992) Crystal structure refinement of osmium(II) disulfide. *Z. Kristallogr.* **202**, 161–162.

Sundby B., Martinez P., and Gobeil C. (2004) Comparative geochemistry of cadmium, rhenium, uranium, and molybdenum in continental, margin sediments. *Geochim. Cosmochim. Acta* **68**, 2485–2493.

Suzuki K., Qi-Lu, Shimizu H., and Masuda A. (1993) Reliable Re–Os age for molybdenite. *Geochim. Cosmochim. Acta* **57**, 1625–1628.

Takahashi Y., Minai Y., Kimura T., Meguro Y., and Tominaga T. (1995) Formation of actinide(III) –humate and its influence on adsorption on kaolinite. *Mat. Res. Soc. Symp. Proc.* **353**, 189–197.

Takahashi Y., Minai Y., Ambe S., Makide Y., Ambe F., and Tominaga T. (1997) Simultaneous determination of stability constants of humate complexes with various metal ions using multitracer technique. *Sci. Total Environ.* **198**, 61–71.

Takahashi Y., Minai Y., and Tominaga T. (1998a) Complexation of Eu(III) with humic substances fractionated by coagulation. *Radiochim. Acta* **82**, 97–102.

Takahashi Y., Kimura T., Kato Y., Minai Y., and Tominaga T. (1998b) Characterization of Eu(III) species sorbed on silica and montmorillonite by leaser-induced fluorescence spectroscopy. *Radiochim. Acta* **82**, 227–232.

Takahashi Y., Minai Y., Ambe S., Makide Y., and Ambe F. (1999) Comparison of adsorption behavior of multiple inorganic ions on kaolinite and silica in the presence of humic acid using the multitracer technique. *Geochim. Cosmochim. Acta* **63**, 815–836.

Tessier A., Campbell P. G. C., and Boisson M. (1979) Sequential extraction procedure for the speciation of particulate trace elements. *Anal. Chem.* **51**(7), 844–851.

Tsunogai S., and Noriki S. (1983) *Kaiyo Kagaku* (ed. M. Nishimura). Sangyo Tosho, Tokyo, 82 pp.

Van Cappellen P., and Wang Y. F. (1996) Cycling of iron and manganese in surface sediments: a general theory for the coupled transport and reaction of carbon, oxygen, nitrogen, sulfur, iron, and manganese. *Am. J. Sci.* **296**, 197–243.

Woodhouse O. B., Ravizza G., Falkner K. K., Statham P. J., and Peucker-Ehrenbrink B. (1999) Osmium in seawater: concentration and isotopic composition vertical profiles in the eastern Pacific Ocean. *Earth Planet. Sci. Lett.* **173**, 223–233.

Zavinsky S. I., Rher J. J., Ankudinov A., Albers R. C., and Eller M. J. (1995) Multiple scattering calculations of X-ray absorption spectra. *Phys. Rev. B* **52**, 2995–3009.

Associate editor: John Crusius

Development of a novel mass spectrometer equipped with an electron cyclotron resonance ion source

Masanori Kidera,[a,*] Kazuya Takahashi,[a] Shuichi Enomoto,[a] Youhei Mitsubori,[b] Akira Goto[a] and Yasushige Yano[a]

[a]Nishina Center for Accelerator-Based Science, RIKEN, 2-1 Hirosawa, Wako, Saitama 351-0198, Japan.
E-mail: Masanori Kidera (kidera@kindex.riken.jp)

[b]Faculty of Engineering Division I, Tokyo University of Science, 1-3 Kagurazaka, Shinjuku-ku, Tokyo 162-8601, Japan

The ionization efficiency of an electron cyclotron resonance ion source (ECRIS) is generally high and all elements can be fundamentally ionized by the high-temperature plasma. We focused our attention on the high potentiality of ECRIS as an ion source for mass spectrometers and attempted to customize a mass spectrometer equipped with an ECRIS. Precise measurements were performed by using an ECRIS that was specialized and customized for elemental analysis. By using the charge-state distribution and the isotope ratio, the problem of overlap, such as that observed in the spectra of isobars, could be solved without any significant improvement in the mass resolution. When the isotope anomaly (or serious mass discrimination effect) was not observed in ECR plasma, the system was found to be very effective for isotope analysis. In this paper, based on the spectrum (ion current as a function of an analyzing magnet current) results of low charged state distributions (2+, 3+, 4+, ...) of noble gases, we discuss the feasibility of an elemental analysis system employing an ECRIS, particularly for isotopic analysis. The high-performance isotopic analysis obtained from an ECRIS mass spectrometer in this study suggests that it can be widely applied to several fields of scientific study that require elemental or isotopic analyses with high sensitivity.

Keywords: ECRIS, mass spectrometer, elemental analysis, isotopic analysis, isotope anomaly

Introduction

A mass spectrometer consists of three essential components—an ion source, a mass analyzer and a detector system. These components have undergone various developments. When a mass spectrometer is used for elemental or isotopic analysis, the ion source technique is very important with regard to its ionic efficiency, stability, etc. Several types of ion source, such as the spark source, glow discharge thermal ionization source and secondary ion source, have been developed for the analyses of inorganic matter and are integrated with mass spectrometry.[1] These ion sources do not have sufficient power for measuring all types of elements and materials. Some ion sources are used only for limited elements and complex and specific chemical procedures for the materials must be analyzed. In recent years, the inductively coupled plasma (ICP) ion source has been commonly used by combining it with various mass analyzers and detector systems. The ICP ion source of the mass spectrometer produces ions by the discharge of Ar gas under atmospheric pressure and offers the following advantages: easy sample introduction, high ionization efficiency for various elements and less interelement and matrix interferences. However, it has the disadvantage that its atmospheric pressure condition requires multiple stages of the vacuum interface system, thereby resulting in a decrease in the transmittance of ions. Another disadvantage is that it yields molecular ions easily. Recently, collision cell technology (CCT) has been developed to avoid interference from molecular ions.[1] However, this technology also leads to a decrease in the transmittance

DOI: 10.1255/ejms.883 ISSN 1469-0667

of ions. Furthermore, the ionization efficiency of the ICP ion source for elements such as Se and As, which have relatively high electronegativity, is not the highest.

In the early 1970s, Geller proposed electron cyclotron resonance ion sources (ECRISs) for the production of highly charged ions.[2] During the past 30 years, these sources have been utilized and the highly-charged ions were enhanced. Many ECRISs are used in heavy-ion accelerators to supply stable beams of heavy ions for various accelerators and users. ECRISs produce stable and intense beams of very highly-charged positive ions from most elements of the periodic table. The ionization efficiency of commonly used ECRISs is high; for example, the ionization efficiency in a general ECR ion source is recognized to be almost 10–20%; furthermore, in the absence of a vacuum device for the plasma chamber, the ionization efficiency is reported to exceed 40% in the case of He, Ne, Ar and Kr.[3] Since 2000, we have been studying the performance of ECRISs in our accelerator facility (RILAC in RIKEN); moreover, we have observed the high performance of the ECRIS, which can work under high vacuum conditions.[4] It is expected that this ECR technology will produce an ion source that can achieve high ionization efficiency for all elements without producing molecular ions and causing interelement and matrix interferences. Further, this technique provides a breakthrough in several fields of scientific study, such as environmental, geochemical or biochemical analyses, by the successful analysis of elements that have not been analyzed with the desired sensitivity and precision by conventional techniques. Based on this feasibility study, we have developed a new mass spectrometer system equipped with an ECRIS. This system is termed as an ECRIS mass spectrometer and the ECRIS was customized for isotopic and elemental analyses. In this paper, we describe this system and introduce the primary data of the isotopic analysis.

The principle of an ECR ion source

An electron in a magnetic field exhibits cyclotronic motion. When this electron and a space electric potential (electric field), which have high frequency (frequencies in the GHz range is used as well) resonates, the electron is accelerated. This is called electron cyclotron resonance (ECR) heating. The relationship between the high frequency and the magnetic field strength at resonance is as follows:

$$Br = 0.0357 \times fc$$

where fc is the frequency [GHz] of a high frequency and Br [T] is the magnetic field strength that causes the resonance.

Further, if an electron enters a magnetic field where the slope of its magnetic strength is sharp, the electron will rebound depending on the conditions. (This phenomenon can be understood from the law of conservation of a magnetic moment.) The electron can be confined by combining the two magnetic fields. The resulting magnetic field is called a mirror magnetic field. If Br exists in the mirror magnetic field, an electron is accelerated sequentially by ECR and becomes a high-temperature electron. ECR plasma is generated by the collision of such a high-temperature electron with a neutral atom or ion. Ions are also confined by a Coulomb force from the electrons while the electrons are confined by the mirror magnetic field. It is very important to note that due to this confinement, the electron confinement time becomes long. Since the electron has a high temperature and its (as well as that of the ion's) confinement time is long, highly-charged ions are produced easily.

R. Geller *et al.* have reported that the charge value, ion beam intensity and beam stability of multicharged ions can be improved rapidly by positioning the multipole magnet to obtain a confinement magnetic field in the radial direction.[2] An ECR ion source with this magnetic field distribution—the so-called minimum-B configuration—is different from an ion source that uses only a mirror magnetic field. Typically, in a cylindrical plasma chamber, the confinement of an axis direction by the mirror magnetic field and the confinement of a radial direction by the multipole magnetic field results in a longer electron confinement time and higher electron density. Hence, the minimum-B type ECR ion source has extremely stable ECR plasma and an intense beam of highly-charged ions is obtained.

Further, ECR plasma in the minimum-B type ECR ion source is generated with a very low gas pressure. For example, when high frequency is introduced in a plasma chamber maintained at a low gas pressure of 1×10^{-4} Pa by using a sample gas, ECR plasma will be produced easily. For the operation of an ECR ion source, the gas pressure and the power of high frequency (if solenoid coils are used for mirror magnetic fields, this is applicable to coil current too) are adjusted by monitoring an ion beam current so that the current reaches maximum and remains stable. An ECR ion source of this minimum-B type is used as the ion source of our ECRIS mass spectrometer.

Equipment for the ECRIS mass spectrometer

As mentioned previously, an ECR ion source with a minimum-B configuration has been commonly used as the ion source in accelerator facilities. In order to generate an intense ion beam of highly-charged ions, the ECR ion sources in these facilities are equipped with a huge magnet and a high-output, high-frequency power supply. Moreover, ions of various elements are generated from samples of various types, for example, gases, metals, oxides, organic compounds, etc. Details of the ion species and the technique of ion production in ECR ion sources can be obtained from Reference 5.

As the first step in the development of the mass spectrometer for elemental and isotopic analyses, the ECR system needed to be customized in a similar way to usual analytical instruments. It was also necessary to design

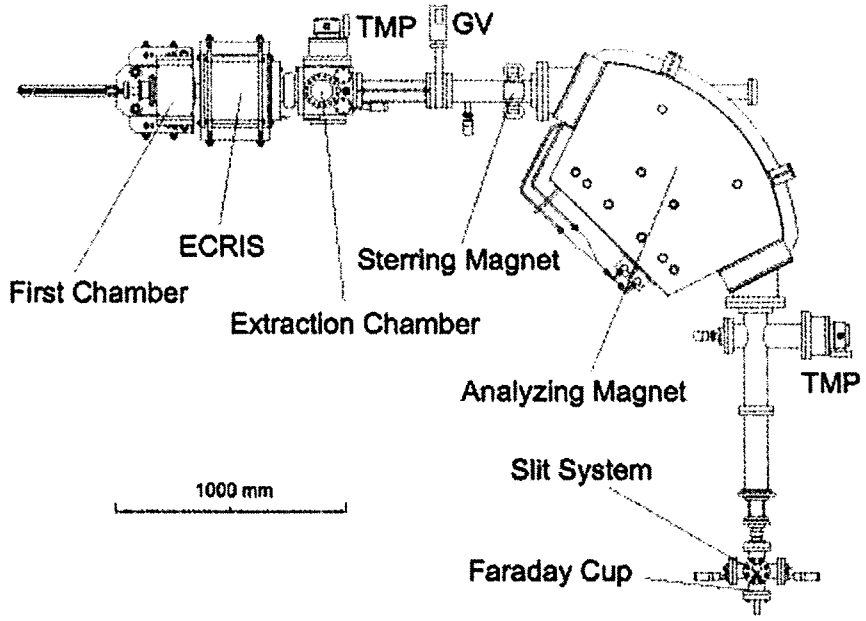

Figure 1. Schematic view of the ECRIS mass spectrometer.

the ion optics and mass analyzer systems for the ECRIS appropriately.

Figure 1 shows a schematic view of the ECRIS mass spectrometer. This system consists mainly of the ECRIS, an analyzing magnet that can focus in a vertical direction (axial focusing) by using the edge angles in the entrance and exit of the magnet and a detection system; these components are described below in detail.

Ion source (ECRIS)

The ECR ion source is the most important component that characterizes the system. The ECRIS primarily consists of the following three parts: permanent magnets for the magnetic mirror field, a high-frequency power supply and a plasma chamber. A magnetic field is produced by the permanent magnets. The permanent magnet unit was manufactured by Shin-Etsu Chemical Co., Ltd. Figure 2 shows a

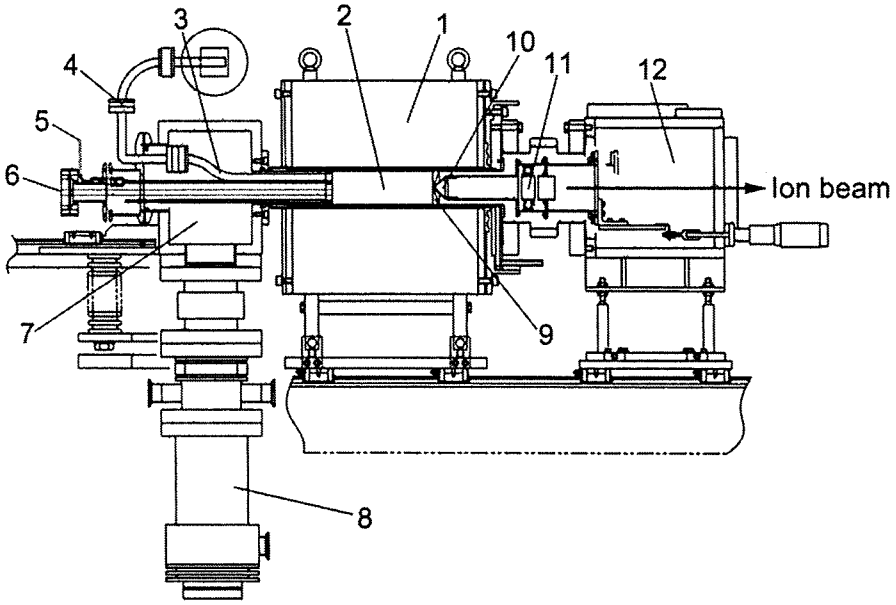

Figure 2. Cross-sectional view of the ECRIS, first chamber and extraction chamber. 1: Permanent magnets (ring magnets and hexapole magnet), 2: plasma chamber, 3: wave guide, 4: quartz pressure window, 5: gas feed, 6: insertion flange for sample, 7: first chamber, 8: turbomolecular pump (220 L min^{-1}), 9: plasma electrode, 10: extraction electrode, 11: Einzel lens and 12: Extraction chamber.